PHILOSOPHICAL TRANSACTIONS A

royalsocietypublishing.org/rsta

CC BY

Research

Cite this article: Keeble J *et al*. 2026 Tropospheric Ozone Assessment Report II: Stratosphere–troposphere exchange of ozone. *Phil. Trans. R. Soc. A* **384**: 20250271.
https://doi.org/10.1098/rsta.2025.0271

Received: 19 January 2026
Accepted: 29 July 2026

One contribution of 8 to a theme issue 'Tropospheric Ozone Assessment Report II'.

Subject Areas:
atmospheric science, atmospheric chemistry

Keywords:
stratosphere–troposphere exchange, tropospheric ozone, tropopause

Author for correspondence:
James Keeble
e-mail: j.keeble2@lancaster.ac.uk

Supplementary material is available online at https://doi.org/10.6084/m9.figshare.c.8658118.

THE ROYAL SOCIETY PUBLISHING

Tropospheric Ozone Assessment Report II: Stratosphere–troposphere exchange of ozone

James Keeble[1], Paul T. Griffiths[2], Marta Abalos[3], Dimitris Akritidis[4,5], Samuel Bartusek[6,7], Owen R. Cooper[8], Qiang Fu[9], Michaela I. Hegglin[10,11,12], Fernando Iglesias-Suarez[13], Gerbrand Koren[14], Oindrila Nath[15,16], Michael Prather[17], Davide Putero[18], Chaitri Roy[19], Bhupendra Bahadur Singh[19], Andreas Stohl[20], Katharina Blazytko[10], Thomas Trickl[21], Oliver Wild[1] and Prodromos Zanis[4]

[1]Lancaster Environment Centre, Lancaster University, Lancaster, UK
[2]School of Chemistry, University of Bristol, Bristol, UK
[3]Department of Earth Physics and Astrophysics, Universidad Complutense de Madrid, Madrid, Community of Madrid, Spain
[4]Department of Meteorology and Climatology, School of Geology, Aristotle University of Thessaloniki, Thessaloniki, Greece
[5]Atmospheric Chemistry Department, Max-Planck-Institut für Chemie, Mainz, Germany
[6]Lamont-Doherty Earth Observatory, Columbia University, Palisades, NY, USA
[7]Department of Earth and Environmental Sciences, Columbia University, New York, NY, USA
[8]NOAA Chemical Sciences Laboratory, Boulder, CO, USA
[9]Department of Atmospheric and Climate Science, University of Washington, Seattle, WA, USA
[10]Institute of Climate and Energy Systems – Stratosphere (ICE-4), Forschungszentrum Jülich, Jülich, Germany
[11]Department of Meteorology, University of Reading, Reading, UK
[12]Institute for Atmospheric and Environmental Research, University of Wuppertal, Wuppertal, Germany
[13]Predictia Intelligent Data Solutions S.L., Santander, Spain
[14]Copernicus Institute of Sustainable Development, Utrecht University, Utrecht, the Netherlands

© 2026 The Authors. Published by the Royal Society under the terms of the Creative Commons Attribution License http://creativecommons.org/licenses/by/4.0/, which permits unrestricted use, provided the original author and source are credited.

Downloaded from royalsocietypublishing.org/rsta/article-pdf/doi/10.1098/rsta.2025.0271/6174200/rsta.2025.0271.pdf
by Karlsruhe Inst of Technology user
on 02 November 2026

[15]Space Physics Laboratory, Vikram Sarabhai Space Centre, Thiruvananthapuram, India
[16]Royal Belgian Institute for Space Aeronomy (BIRA-IASB), Uccle 1180, Belgium
[17]Earth System Science Department, UC Irvine, Irvine, USA
[18]National Research Council of Italy – Institute of Atmospheric Sciences and Climate, CNR–ISAC, Turin, Italy
[19]Indian Institute of Tropical Meteorology, Ministry of Earth Sciences, Pune, India
[20]Department of Meteorology and Geophysics, University of Vienna, Josef-Holaubek-Platz 2, 1090 Vienna, Austria
[21]Karlsruher Institut für Technologie, IMK-IFU, Kreuzeckbahnstr. 19, 82467 Garmisch-Partenkirchen, Germany

JK, 0000-0003-2714-1084; DP, 0000-0002-9721-1036

Stratosphere–troposphere exchange (STE) of ozone is a significant source of tropospheric ozone, influencing air quality, atmospheric chemistry and climate forcing. This assessment synthesizes recent advances in understanding the magnitude, mechanisms, variability and future evolution of ozone transport across the tropopause, updating earlier reviews using observations, reanalyses and global chemistry–climate models. Globally, monthly mean STE is driven by the large-scale circulation of the stratosphere, but on shorter time scales and synoptic scales episodic dynamical processes such as tropopause folds, cutoff lows and wave breaking are locally important. Based on a synthesis of published estimates for 2000–2020, the present-day global net STE of ozone is assessed to be 380 (350–450) Tg O_3 yr^{-1}. This net flux is composed of a strong downward transport from the stratosphere into the troposphere of approximately 540 Tg O_3 yr^{-1} in the extratropics, partially offset by an upward transport of ozone from the troposphere into the stratosphere of about 190 Tg O_3 yr^{-1} in the tropics. Around 60% of the downward extratropical transport occurs in the Northern Hemisphere. STE exhibits pronounced seasonality as well as interannual variability linked to climate modes including the El Niño–Southern Oscillation (ENSO) and the Quasi-Biennial Oscillation (QBO). Analyses indicate a decline in STE of 2.7% $decade^{-1}$ during the late twentieth century associated with ozone depletion, while future projections consistently project an increase in STE of around 4.7% $decade^{-1}$ as global circulation responds to climate change and stratospheric ozone recovers.

This article is part of the theme issue 'Tropospheric Ozone Assessment Report II'.

1. Introduction

Stratosphere–troposphere exchange (STE) refers to the two-way transport of air masses and their chemical constituents across the tropopause. This exchange chemically connects the ozone-rich stratosphere with the troposphere, and as a result, STE is a significant contributor to the tropospheric ozone budget, influencing both air quality and radiative forcing. Throughout the remainder of this assessment, STE is used specifically to refer to the transport of ozone across the tropopause unless otherwise stated.

Mass-budget estimates indicate that approximately 21–26 Tg of air enters the lowermost stratosphere through the tropical tropopause region each second, with a comparable compensating return transport in the extratropics [1,2]. However, estimates of cross-tropopause mass transport vary substantially depending on the definition of the tropopause, the diagnostic approach and the treatment of transient recrossing events [3,4]. Air masses are predominantly transported upward from the troposphere into the stratosphere in the tropics, and downward from the stratosphere into the troposphere in the extratropics. The net effect of this transport is a substantial downward flux of ozone into the troposphere, with current estimates suggesting that STE contributes 336–535 Tg O_3 yr^{-1} to the troposphere [1,2,5–8]. However, despite decades of research, large uncertainties remain in quantifying the magnitude, spatiotemporal variability

Downloaded from royalsocietypublishing.org/rsta/article-pdf/doi/10.1098/rsta.2025.0271/6174200/rsta.2025.0271.pdf
by Karlsruhe Inst of Technology user
on 02 November 2026

and trends of STE (e.g. [9,10]), reflecting limited direct observations, uncertainty in reanalyses and substantial inter-model spread.

While STE was noted in the first phase of the Tropospheric Ozone Assessment Report (TOAR) [8,9], the most recent comprehensive review dates back to Stohl *et al.* [11], highlighting the need for an updated synthesis in light of recent advances. This contribution to TOAR-II assesses the role of STE as a source of tropospheric ozone by synthesizing the current state of knowledge, summarizing recent findings and identifying ongoing challenges. Specifically, we address the following questions: (1) What are the methods used to quantify STE, and how do they compare? (2) What is the net annual STE flux of ozone under present-day conditions? (3) What is the magnitude and cause of interannual variability in STE? (4) How is STE likely to evolve in the future? (5) What is the impact of STE on the tropospheric ozone budget and burden?

Throughout this assessment, we follow the terminology proposed by Stohl *et al.* [11]: stratosphere-to-troposphere transport (STT) and troposphere-to-stratosphere transport (TST) refer to one-way fluxes across the tropopause, while STE is defined as the net difference (STE = STT – TST). Under this convention, a positive STE value indicates a net influx of ozone into the troposphere from the stratosphere. Reported STE values are rounded to two significant figures unless otherwise stated. Following TOAR-II terminology recommendations, mixing ratios are expressed in nmol mol^{-1}, with 1 nmol mol^{-1} equivalent to 1 ppb.

2. The tropopause

Any assessment of STE must consider the tropopause, which marks the boundary between the troposphere, where turbulence and convection cause relatively rapid air mass mixing, and the more stably stratified stratosphere, where transport and mixing processes are slow. The altitude of the tropopause varies with latitude: it is highest in the tropics (approx. 16–17 km), lowest near the poles (approx. 8 km) and drops sharply in the subtropics, forming a feature known as the 'tropopause break' [12]. Rather than being a sharp boundary, the tropopause represents a transition region, spanning several hundred metres to a few kilometres in depth (e.g. [13,14]). Its structure is often deformed by synoptic-scale dynamics such as Rossby wave breaking, forming tropopause folds that facilitate exchange across this boundary [15–18]. The tropopause is formally defined by the World Meteorological Organization ([19]) using a thermal lapse-rate criterion. In practice, however, a range of diagnostic criteria based on temperature, dynamics or chemical composition have been widely used to identify the transition between the troposphere and stratosphere:

— Temperature-based definitions include the widely used lapse-rate tropopause [19], calculated from the vertical temperature gradient and the cold-point tropopause. While the lapse-rate tropopause is applicable across most latitudes, it can be undefined in polar regions during winter because the required lapse-rate criterion is not satisfied owing to the vertical temperature structure of the polar lower stratosphere [20]. In addition, temperature-based definitions may misidentify features such as folds, and multiple tropopauses can occur [21].
— Dynamical-based definitions use potential vorticity (PV) surfaces to identify the tropopause. Common thresholds range from approximately 1 to 5 PV units (PVU). A value of 2 PVU is widely used as the extratropical dynamical tropopause [12,17], while a threshold of approximately 3.5 PVU has been shown to provide a closer approximation to the extratropical thermal tropopause (e.g. [22,23]). PV-based definitions are particularly useful for identifying tropopause folds and stratospheric intrusions because PV is conserved under adiabatic conditions and can therefore represent the tropopause as a material surface [24]. However, the applicability of PV-based tropopause definitions is limited in the tropics. The PV-gradient tropopause introduced by Kunz *et al.* [25], which identifies the tropopause from the maximum PV gradient rather than a fixed PV threshold, better captures the tropopause structure

Downloaded from royalsocietypublishing.org/rsta/article-pdf/doi/10.1098/rsta.2025.0271/6174200/rsta.2025.0271.pdf
by Karlsruhe Inst of Technology user
on 02 November 2026

near the subtropical jets. In the deep tropics, however, the reversal of planetary vorticity across the equator causes PV to change sign and PV contours become vertical, limiting the ability of PV-based approaches to provide a meaningful tropopause definition.

— Composition-based definitions use sharp changes in trace gases such as ozone, carbon monoxide (CO), nitrous oxide (N_2O) and total odd nitrogen (NOy) to identify the tropopause. While single-tracer thresholds (e.g. the 150 nmol mol^{-1} ozonopause) can approximate the tropopause [12,26], tracer–tracer relationships (e.g. ozone–CO or NOy–N_2O) more robustly identify the transition layer [27]. Idealized model tracers such as e90 [14] can also be used, but lack observational analogues.

No single tropopause definition is best for all applications, and the range of definitions outlined above will continue to be used according to the region of interest and data availability. However, this range of definitions poses a challenge for comparing STE estimates across the literature. Global STE flux estimates have been shown to be sensitive to the tropopause definition applied [10,20,28], with differences of up to 30 Tg O_3 yr^{-1} (approx. 8%) reported [29].

3. Transport across the tropopause

The global pattern of STE is controlled primarily by the Brewer–Dobson circulation (BDC), the large-scale overturning circulation that transports air through the stratosphere [17]. Tropospheric air enters the stratosphere in the tropics, rises, moves towards the poles and eventually descends back into the troposphere at higher latitudes. The net global STE ozone flux therefore consists of a large positive STT term in the extratropics, partially offset by a smaller, negative TST term in the tropics. However, this distinction between extratropical STT and tropical TST represents a global, long-term mean description and does not capture all exchange pathways. For example, westerly ducts in the subtropics can provide pathways for stratospheric air to penetrate into the tropical region [30,31]. Seasonal variations in tropopause height and stratospheric circulation strength imprint a pronounced annual cycle on extratropical net STT fluxes [1,2,32].

While the BDC constrains the global STE flux on seasonal to interannual time scales, STT at regional and local scales is dominated by episodic events that persist for several days [11,33]. Important synoptic-scale mechanisms contributing to STT include cutoff lows and tropopause folds. Cutoff lows are isolated upper-level cyclonic circulations that can transport stratospheric air downward through gradual isentropic descent, with subsequent mixing into the troposphere [34–37]. Tropopause folds are large-scale deformations of the tropopause that typically form near bends in the polar or subtropical jet streams. Within these folds, dry, ozone-rich stratospheric air descends along isentropic surfaces into the trailing anticyclonic region of large-scale weather systems [15,17,38–42]. These intrusions can contribute substantially to local enhancements in tropospheric ozone. However, not all ozone enhancements associated with tropopause folds represent irreversible STT; a substantial fraction of the ozone-rich air may remain within or return to the stratosphere [30]. Smaller-scale processes, such as gravity-wave breaking, contribute to localized turbulent mixing and irreversible transport across the tropopause [43–46]. Localized STT driven by deep convection has also been observed and modelled ([21,47,48]). The episodic nature of STT events introduces substantial uncertainty into ozone flux estimates derived from observations.

Observations indicate that transport within folds occurs in thin, filamentary layers [43,49–52], which, under the right circumstances, can penetrate into the middle troposphere, accounting for a substantial fraction of ozone-rich air in the free troposphere (e.g. [53–55]). Figure 1a shows the ozone mixing ratios in a cross-section through a fold captured by the Copernicus Atmosphere Monitoring Service (CAMS) reanalysis [57], highlighting the substantial increase in ozone present within the fold compared to the surrounding tropospheric air. Also shown is a map of mid-tropospheric ozone, which highlights the elongated filaments with elevated mixing ratios that frequently co-locate with diagnosed tropopause folds (figure 1b). However, not all regions of high

Downloaded from royalsocietypublishing.org/rsta/article-pdf/doi/10.1098/rsta.2025.0271/6174200/rsta.2025.0271.pdf
by Karlsruhe Inst of Technology user
on 02 November 2026

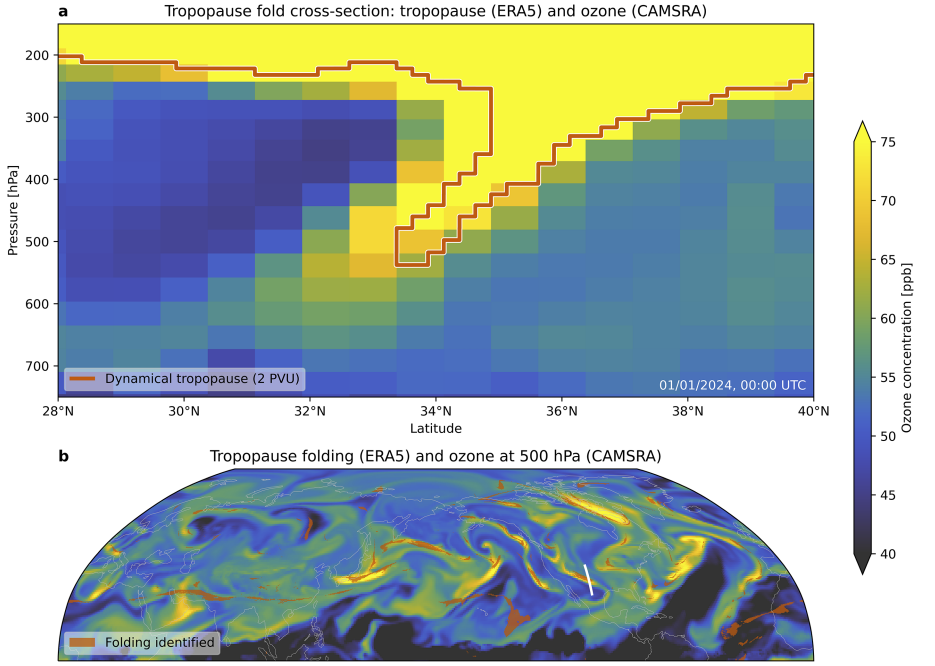


Figure 1. (a) Cross-section of a tropopause fold along a latitudinal cross-section (white line in panel b) on 1 January 2024. The orange line shows the dynamical tropopause in ERA5, while the shading shows ozone mixing ratios from CAMS reanalysis. (b) Map of ozone at 500 hPa from the CAMS reanalysis (shading) and columns in which tropopause folding was identified (orange) using the method of Bartusek *et al.* [56], during the same time step. Both panels represent conditions at 00:00 UTC on 01 January 2024.

ozone mixing ratios correspond to regions where folds have been diagnosed at the same time, although some of these ozone enhancements may persist from folds that have already terminated.

Climatologies of tropopause fold frequency derived from reanalysis datasets demonstrate that tropopause folding varies strongly with season and latitude (figure 2). Shallow folds are common near the subtropical jet streams, while medium and deeper folds are closely associated with mid-latitude storm tracks. In terms of frequency, shallow folds are most common, while medium and deep folds are rarer by approximately an order of magnitude. However, medium and deep folds have a greater potential to contribute to local STT because they penetrate farther into the troposphere and are more likely to undergo irreversible mixing into the surrounding troposphere air, whereas shallow folds often remain near the tropopause and may return to the stratosphere.

Very deep folds can influence near-surface ozone in regions such as the eastern Mediterranean and Middle East [59,60], western United States ([61–64]), and the Tibetan Plateau [54,65,66]. While models with $1° \times 1°$ horizontal resolution have been shown to capture large-scale tropopause folds [33,67,68], the vertical resolution needed to represent these structures accurately remains uncertain [40,69,70], and accurately resolving the fine-scale morphology of folds may require horizontal resolutions finer than 50 km [56]. While modern reanalyses are generally able to diagnose the occurrence and large-scale structure of tropopause folds, the spatial resolution of these folds makes them an ongoing challenge for free-running global climate models to capture.

A further mechanism for STT is deep convection associated with mesoscale convective systems and tropical cyclones, which can affect upper-tropospheric ozone in the vicinity of these systems. In intense cases, convective updrafts may penetrate or strongly interact with the lower stratosphere, entraining stratospheric air that is subsequently transported into the upper troposphere [48,71–74]. However, such events are rare, highly localized and episodic, and their contribution to the global STE budget is probably small when averaged over longer time scales. The extent to

Downloaded from royalsocietypublishing.org/rsta/article-pdf/doi/10.1098/rsta.2025.0271/6174200/rsta.2025.0271.pdf
by Karlsruhe Inst of Technology user
on 02 November 2026

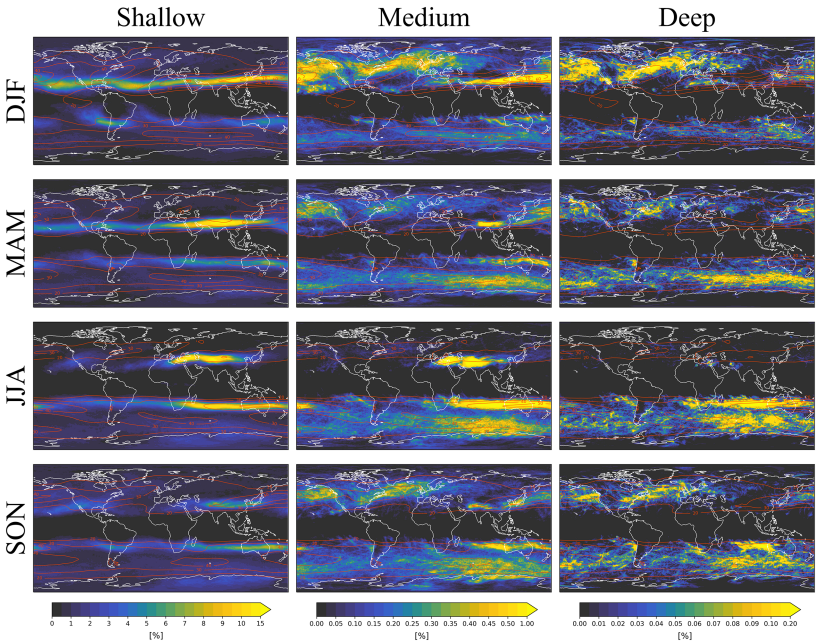


Figure 2. Mean seasonal frequency (%) of shallow, medium, and deep tropopause folds identified in the MERRA-2 reanalysis for the period 2003–2018 using the method of Akritidis *et al.* [58]. Fold frequency is defined as the percentage of time steps each season in which a tropopause fold is diagnosed at each grid box. Red contours denote a minimumhorizontal wind speed of 20 m s^{-1} at 250 hPa. Note the different colour scales used for shallow, medium and deep folds, reflecting their differing relative frequencies of occurrence.

which deep convective transport influences surface and near-surface ozone remains highly uncertain and is an active area of discussion in the literature ([74–76]).

4. Observational constraints on *in situ* tropospheric ozone with a stratospheric origin

Observations consistently demonstrate that stratospheric ozone significantly contributes to tropospheric ozone mixing ratios, though the magnitude varies strongly by region, season and altitude. The utility of satellite observations for isolating STT contributions is limited by vertical resolution and retrieval uncertainties [77]. Consequently, most quantitative observation-based estimates rely on measurements of species indicative of STT (e.g. O_3, water vapour (H_2O), N_2O and cosmogenic radionuclides) obtained from surface-based instruments, sondes, lidars or aircraft (e.g. [78]).

As already discussed, filaments of ozone with a stratospheric origin can persist in the troposphere for up to two weeks (Trickl *et al*. [79]), during which time they may either return to the lower stratosphere or undergo irreversible mixing with the surrounding tropospheric air [80,81]. This complicates the quantification of STT contribution to lower tropospheric and near-surface ozone, except during direct and intense deep intrusion events. Numerous studies document large ozone enhancements from stratospheric intrusions, occasionally reaching the surface during rare, deep events ([51,82–88]).

Over northeastern North America, ozonesonde observations in 2004 indicated that STT contributed approximately 20%–25% of the seasonal mean tropospheric ozone column during July–August [89]. Complementary analyses across 18 North American sites show a similar average stratospheric influence in the middle and upper troposphere [90], while spring tropopause-fold events can produce substantial episodic enhancements of background tropospheric ozone [88].

Downloaded from royalsocietypublishing.org/rsta/article-pdf/doi/10.1098/rsta.2025.0271/6174200/rsta.2025.0271.pdf
by Karlsruhe Inst of Technology user
on 02 November 2026

Analysis of radionuclides at Alert, Canada, indicates that STT stratospheric inputs can account for a maximum of 10%–15% of the ozone locally at the surface in spring and for less during the rest of the year [91]. During the TOPSE campaign, ^{7}Be observations combined with O_3 and HNO_3 identified stratospherically influenced air throughout the northern North American free troposphere, predominantly above 6 km but extending to lower altitudes at high latitudes [91]. GEOS-5 simulations during DISCOVER-AQ also identified frequent summertime stratospheric intrusions over Maryland, including events that penetrated into the lower troposphere and enhanced surface ozone (Ott *et al*. [92]). In Europe and the Himalayas, frequent winter–spring intrusions account for up to 25% of near-surface ozone mixing ratios, with high-elevation sites recording intrusion frequencies of 5%–17% [67,93–96], while analysis of radionuclides at the high-elevation stations of Jungfraujoch and Zugspitze indicated average annual stratospheric ozone percentage contributions on near-surface ozone of approximately 6.5% and 5%, respectively [97]. Later studies, based on revised tracer correlations, found much higher stratospheric contributions to the Zugspitze ozone, responsible for the positive ozone trend at this mountain site since the 1980s [51]. Similar events have been reported at Mt. Bachelor in the northwestern United States [98]. Over southern Africa, STE events identified from ozonesonde observations over Irene are most frequent during winter and spring and are typically restricted to the upper troposphere, with only occasional intrusions into the mid-troposphere and negligible impacts at the surface [99]. In East Asia, STT contributes substantially to seasonal and episodic ozone variability. For example, over the Tibetan Plateau, where the high elevation favours STT, up to 20% of the springtime tropospheric ozone column has been attributed to stratospheric air [100], while long-term ozonesonde records across China and the northwestern Pacific show persistent upper-tropospheric enhancements and rising ozone trends partly linked to STT [101,102]. Lidar and balloon soundings complement these records by capturing the vertical structure of intrusions [51,79,103–106]. Most studies confirm that only a subset of deep events penetrate below 3 km (e.g. [103]).

Recent analyses provide further observational evidence that stratospheric processes influence ozone distributions across the upper troposphere–lower stratosphere (UTLS). Using a combination of aircraft observations, ozonesondes and reanalysis products, [107] identified persistent hemispheric differences in UTLS ozone, with lower ozone concentrations in the Southern Hemisphere associated with the impact of severe stratospheric ozone depletion. Their analysis also showed that dynamical disturbances, including sudden stratospheric warming events, can substantially modify ozone distributions within the STE region. These findings reinforce the importance of considering hemispheric differences in stratospheric ozone availability and dynamical variability when interpreting observations of ozone transport into the troposphere.

Overall, observations demonstrate that STE is an important contributor to tropospheric ozone variability across both hemispheres, with contributions most evident in spring and in mountainous regions. However, the regional climatology of STE remains poorly constrained owing to sparse measurements over the oceans and the Southern Hemisphere, and currently there is no feasible way to directly observe the global STE flux. Importantly, none of these individual sites or studies can constrain the global STE flux, but together they provide compelling evidence that STE exerts a strong and widespread influence on tropospheric ozone.

5. Methods for quantifying stratosphere–troposphere exchange

Because air crossing the tropopause cannot be observed directly on global scales, global STE must be inferred using a variety of observational and modelling techniques, each with distinct advantages, limitations and applications. To date, no single study has systematically compared these methods within a common framework (e.g. using the same model or reanalysis dataset). As a result, it remains difficult to determine the extent to which differences in published STE estimates reflect genuine methodological differences rather than differences in the underlying data or model configuration. The principal methods are summarized below.

Downloaded from royalsocietypublishing.org/rsta/article-pdf/doi/10.1098/rsta.2025.0271/6174200/rsta.2025.0271.pdf
by Karlsruhe Inst of Technology user
on 02 November 2026

(a) Mass budget method

The lowermost stratosphere mass budget method, pioneered by Appenzeller *et al.* [32], has been widely used to quantify air mass and ozone STE (e.g. [2,23,29,108,109]). These studies used the 380 K isentropic surface as the upper boundary of the lowermost stratosphere, with the extratropical lapse-rate tropopause defining its lower boundary. A key strength of this method is its ability to provide separate regional flux estimates (e.g. Northern Hemisphere, Southern Hemisphere, extratropics, tropics and global totals), making it particularly useful for diagnosing latitudinal differences in STE. More recently, Wang *et al.* [110] proposed replacing the fixed 380 K surface with a dynamically varying isentropic surface that accounts for changes in the height of the tropical tropopause. They showed that this refinement is important when estimating STE under substantially different climate states, such as the Last Glacial Maximum. In contrast, STE estimates are largely insensitive to the definition of the extratropical tropopause [1]. While this method accurately estimates net air mass fluxes over regional and global scales, it cannot identify the locations or magnitudes of individual STE events because it relies on integrated mass budgets rather than tracking individual air parcels.

(b) Tracer–tracer correlations

Tracer–tracer methods quantify STE using relationships between ozone and long-lived tracers with distinct stratospheric signatures, such as nitrous oxide (N_2O), sulfur hexafluoride (SF_6) and PV. Their approximately linear relationships in the lower stratosphere allow observed ozone–tracer correlations to be combined with tracer fluxes across the tropopause to constrain the ozone STE flux. Radioactive isotopes have also been used for this purpose. Following nuclear bomb tests in the 1950s and 1960s, ^{90}Sr was used to infer large-scale exchange rates [16]. More recently, cosmogenic isotopes such as ^{35}S have been used to detect deep stratospheric intrusions and associated ozone enhancements [111], while the $^{10}Be/^{7}Be$ ratio has been used to identify stratospheric intrusions and quantify their contribution to tropospheric ozone (e.g. [97,112]). In addition, improvements in measurements of ^{17}O-excess in CO_2 now make this tracer increasingly viable for constraining STE (e.g. [113,114]). A key advantage of tracer-based methods is their applicability to both *in situ* observations and global model output. However, they assume that tracer–ozone relationships established in the lower stratosphere remain largely conserved during transport, an assumption that can be weakened by chemical processing and sub-grid-scale mixing.

(c) Lagrangian trajectory modelling

Lagrangian trajectory methods diagnose STE by following air parcels through space and time as they cross the tropopause using meteorological fields from reanalyses or forecast models. This approach provides detailed information on transport pathways, residence times and exchange depths [115]. After the pioneering studies of Reed [18], Staley [116] and Danielsen [15], trajectory methods have been widely applied to both individual case studies and long-term climatologies (e.g. [11,36,115,117]). More recent studies combine trajectories with reanalysis data, chemical tracers and high-resolution modelling to diagnose STE across regional and global scales [64,95,118]. A key strength of this approach is its ability to resolve the fine-scale filamentary structures generated by atmospheric transport that are often smoothed in Eulerian diagnostics. It also distinguishes between shallow, transient exchange events and deeper, more chemically significant intrusions (e.g. [52,119]). However, results depend strongly on the quality of the driving wind fields and the chosen integration time. Simple trajectory models follow individual air parcels without accounting for mixing, whereas Lagrangian particle dispersion models represent turbulent and convective mixing by following ensembles of particles. Furthermore, estimated one-way air mass fluxes depend on the smallest spatial and temporal scales resolved by the model (e.g. [4,120,121]).

Downloaded from royalsocietypublishing.org/rsta/article-pdf/doi/10.1098/rsta.2025.0271/6174200/rsta.2025.0271.pdf
by Karlsruhe Inst of Technology user
on 02 November 2026

(d) Ozone chemical budget approaches

STE can also be inferred from the tropospheric ozone budget, expressed as ΔO_3 = Prod − Loss + STE − Dep, where Prod is chemical production, Loss is chemical loss, and Dep is surface deposition. Rearranging this equation allows STE to be estimated as the residual after the other budget terms are quantified. By construction, this residual represents the global net STE flux, making the method readily applicable within global chemistry–climate models (e.g. [5,8]). However, the method is applicable only in models because most ozone budget terms cannot be directly observed. Accurate estimation requires complete diagnosis of chemical production (approx. 5000 Tg O_3 yr^{-1}), chemical loss (approx. 4500 Tg O_3 yr^{-1}), and deposition (approx. 1000 Tg O_3 yr^{-1}; e.g. [8]). Because STE is obtained as the residual of these much larger terms, any unaccounted-for production or loss is incorrectly attributed to STE. This has proven problematic in recent model intercomparisons where requested diagnostics include only subsets of the full chemical mechanism (e.g. CMIP6 diagnostics). While some studies report good agreement between residual and transport-derived STE estimates (e.g. [122]), others find substantial differences (e.g. [110]), probably reflecting incomplete chemical diagnostics and methodological differences. A potential approach to reduce this problem is to diagnose the net chemical ozone tendency directly rather than diagnosing production and loss separately.

(e) Eulerian diagnostic approaches

The Eulerian diagnostic developed by Wei [123] estimates STE by computing transport across the tropopause surface directly within gridded model space. Its principal advantage is that it can be applied directly in chemistry–climate and Earth system models without trajectory calculations. However, the method estimates the relatively small net STE flux as the difference between much larger upward (TST) and downward (STT) transport terms, making it highly sensitive to numerical errors. In addition, numerical diffusion across the sharp gradients in tracer concentrations and meteorological fields near the tropopause can introduce spurious cross-tropopause transport [124]. Although improvements have been proposed (e.g. [30]), Eulerian diagnostics remain less widely used than alternative approaches.

6. Tagged tracer methods

Rather than diagnosing transport across the tropopause directly, tagged tracer approaches such as O_3S (stratospheric ozone tracer) estimate the contribution of stratospheric ozone by following ozone that originated in the stratosphere after it enters the troposphere; O_3S has been widely used in global models to quantify the influence of stratospheric ozone on tropospheric ozone (e.g. [125–128]). In many implementations, ozone is tagged throughout the stratosphere and transported into the troposphere by the model circulation. Once in the troposphere, O_3S undergoes only a prescribed chemical loss and does not include *in situ* photochemical production [129]. Tagged tracers are attractive because they avoid explicitly diagnosing fluxes across the tropopause and provide a three-dimensional picture of stratospheric influence throughout the troposphere. They have therefore been widely used to investigate future changes in STE associated with declining ozone-depleting substances (ODS) and increasing greenhouse gases (GHGs) (e.g. [59,125,126,130]). Recent studies report increasing O_3S at high latitudes under future scenarios, attributed to enhanced STE and stratospheric ozone recovery [131].

Despite their widespread application, tagged tracers have important limitations. Because the tracer retains its stratospheric label throughout transport, it continues to be counted as stratospheric ozone even after extensive mixing with tropospheric air and chemical processing, potentially overestimating the influence of STT on tropospheric and surface ozone [132]. Tagged tracers also assume that stratospheric ozone behaves as a passive tracer after entering the

Downloaded from royalsocietypublishing.org/rsta/article-pdf/doi/10.1098/rsta.2025.0271/6174200/rsta.2025.0271.pdf
by Karlsruhe Inst of Technology user
on 02 November 2026

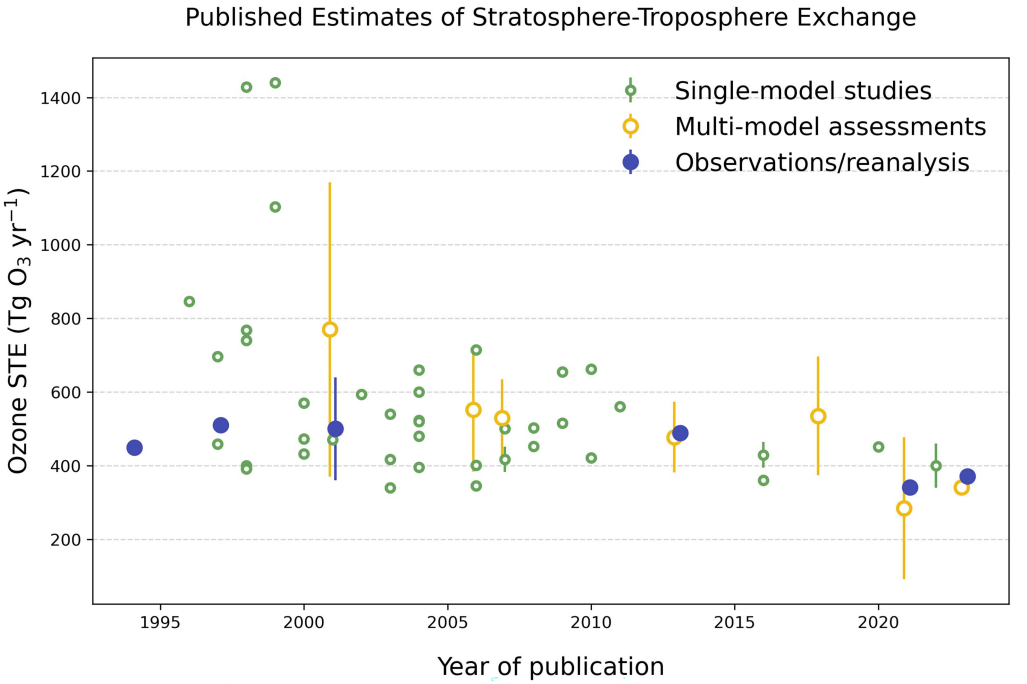


Figure 3. Published estimates of STE of ozone as a function of publication date. Green circles represent single model studies, yellow circles represent multi-model assessments and blue dots represent estimates derived from observations/reanalysis datasets. Specific publications and datasets used in this figure are available in the supplementary material, supplementary table 1.

troposphere and therefore do not represent the changes in tropospheric photochemistry that occur when additional ozone modifies chemical production and loss rates. In addition, air parcels that briefly enter the stratosphere can acquire the O_3S label before rapidly returning to the troposphere, leading to possible double counting. For these reasons, tagged tracers are best interpreted alongside complementary STE diagnostics.

No single method is optimal for all applications. Mass-budget approaches provide the most direct estimates of global net STE, trajectory methods are best suited for diagnosing individual exchange events and pathways, tracer-based approaches provide strong observational constraints, while tagged tracers quantify the influence of stratospheric ozone within the troposphere rather than the flux itself. Consequently, comparisons between published STE estimates should consider both the underlying methodology and the associated tropopause definition.

7. Quantifying global stratosphere–troposphere exchange under present-day conditions

Attempts to quantify the contribution of STE to tropospheric ozone date back to the 1960s (e.g. [133,134]), reflecting long-standing scientific interest. In the decades since, numerous studies have estimated STE using a range of approaches, including single-model simulations, multi-model intercomparisons, chemical budget analyses and observation-based methods (figure 3). Reported values span a wide range, from approximately 300 to 1400 Tg O_3 yr^{-1}. Early model-derived estimates, particularly from the 1990s, often yielded higher values and showed poor agreement across studies, whereas more recent work has tended to converge toward 350–600 Tg O_3 yr^{-1}. Note that the figure shows STE estimates by publication year, which may not correspond to the year the STE value was actually calculated. The apparent decline in model-derived STE estimates

Downloaded from royalsocietypublishing.org/rsta/article-pdf/doi/10.1098/rsta.2025.0271/6174200/rsta.2025.0271.pdf
by Karlsruhe Inst of Technology user
on 02 November 2026

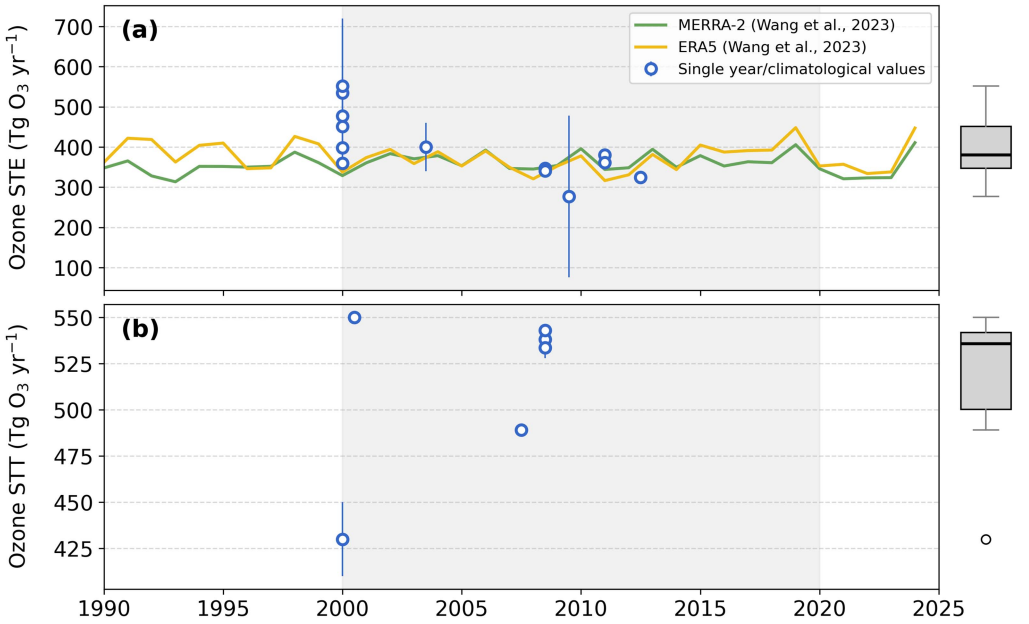


Figure 4. Published estimates of ozone STE (upper panel) and ozone STT (lower panel). The grey shaded region indicates the period (2000–2020) over which published estimates were used to derive the values presented in this assessment. Blue circles show individual published estimates, including single-year and climatological values. Box-and-whisker plots summarize the distribution of available estimates, showing the median and interquartile range. The green and yellow lines show annual mean estimates of ozone STE derived from MERRA-2 and ERA5, respectively. Note that the ordinate ranges differ between the two panels to accommodate the available estimates and improve readability. Specific publications and datasets used in this figure are provided in supplementary material, in supplementary tables 2 and 3.

probably reflects improvements in the models, including increased horizontal and vertical resolution, improved representation of chemistry and transport processes and differences in diagnostic approaches. These structural changes are probably more important than any real change in atmospheric STE.

In contrast to model estimates, observation-based constraints have consistently given global STE values of 400–600 Tg O_3 yr^{-1} (e.g. [29,30,108,109,135–137]). However, these estimates focused on extratropical downward fluxes and did not account for the compensating upward flux of ozone in the tropics [2]. As a result, they systematically overestimated the net transport of stratospheric ozone into the troposphere, with recent studies showing that the tropical upward ozone flux offsets approximately 35% of the extratropical downward flux [1,2,138].

For this assessment, a present-day (2000–2020) estimate of global STE and STT is derived by combining published values restricted to this period (figure 4). Where longer records are available, only the portion covering 2000–2020 is used. This approach combines estimates from single-model studies [5,110,126,139,140], multi-model ensembles [8,28,122,138,141], observation-derived analyses ([1,2]) and reanalysis-based estimates [6,7].

Note that the published STE estimates used here are derived using a number of the methodologies discussed earlier in this assessment. As a result, the spread in published values reflects not only real changes in the atmosphere, but also differences in how STE is quantified, including the sampling period, simulated atmospheric state and methodological differences in how STE is diagnosed. These differences may introduce systematic, method-dependent deviations, although to date no study has compared the broad range of methods used to calculate STE in a single model framework. For example, some of the spread in figure 4 can be attributed to known limitations of specific methodologies. In particular, ozone chemical budget approaches that diagnose

Downloaded from royalsocietypublishing.org/rsta/article-pdf/doi/10.1098/rsta.2025.0271/6174200/rsta.2025.0271.pdf
by Karlsruhe Inst of Technology user
on 02 November 2026

STE as a residual term are prone to systematic uncertainty. Notably, both the highest and lowest STE values shown in figure 4 are derived from multi-model studies that use the ozone chemical budget approach. This limitation has been well documented for CMIP6 models, where incomplete ozone budget diagnostics lead to substantial model–model variability in residual-based STE estimates [5]. The synthesis presented here therefore represents a pragmatic assessment of the range of values presented in the existing literature, rather than a harmonized intercomparison of equivalent STE fluxes, and the resulting best-estimate values should be interpreted in this context.

To mitigate these methodological limitations, this assessment combines STE estimates derived from models, reanalyses and observation-based approaches. By drawing on multiple independent data sources, this synthesis reduces reliance on any single dataset or diagnostic framework and reduces susceptibility to biases associated with individual methodologies. While differences between approaches remain, the broad agreement across fundamentally different lines of evidence increases confidence that the resulting estimate provides a robust representation of the present-day atmospheric STE flux, rather than being dominated by the assumptions of any individual methodology. To limit the influence of outliers, the median and interquartile range (IQR) of the combined distribution of published estimates are reported, with all estimates weighted equally regardless of approach. Equal weighting is adopted because the uncertainty associated with methodological differences cannot currently be quantified robustly. Based on this methodology, the present-day best estimate of global STE is 380 (IQR: 350–450) Tg O_3 yr^{-1}, while global STT is 540 (IQR: 500–540) Tg O_3 yr^{-1}. To avoid implying unwarranted precision, all values reported in this section are given to two significant figures.

Regional breakdowns reveal a pronounced hemispheric asymmetry in STE. The extratropics account for nearly all of the downward flux, approximately 540–570 Tg O_3 yr^{-1}, with a larger contribution from the Northern Hemisphere (310–330 Tg O_3 yr^{-1}) than from the Southern Hemisphere (210–250 Tg O_3 yr^{-1}), consistent with stronger wave activity and a more vigorous BDC in the north (e.g. [1,2,6,29,109,135]). In contrast, the tropics exhibit a net upward flux of approximately 180–200 Tg O_3 yr^{-1} [1,2,138]. STE also displays a strong seasonal cycle. Downward extratropical fluxes peak in spring, driven by rising tropopause height, enhanced baroclinic activity and increased tropopause folding, while tropical variability is comparatively weak [2,29,109,142,143]. Consequently, the global STE seasonal cycle closely follows that of the extratropics, with a maximum in boreal spring and a secondary maximum in austral spring.

8. Drivers of stratosphere–troposphere exchange variability

STE exhibits strong interannual and decadal variability linked to natural climate modes and episodic disturbances, which alter large-scale circulation (e.g. the BDC), jet-stream strength and position, planetary-wave activity and tropopause structure, thereby modulating the flux of ozone into the troposphere. Understanding these connections is critical for interpreting observed variability in tropospheric ozone and for constraining the predictability of STE-related ozone fluxes.

El Niño–Southern Oscillation (ENSO) exerts the most prominent effect. During El Niño, enhanced convection and diabatic heating in the tropical upper troposphere modify the subtropical jets and associated wave dissipation, which results in a strengthening of the shallow branch of the BDC [144]. This increase in tropical lower-stratospheric upwelling reduces ozone concentrations through the enhanced transport of ozone-poor tropospheric air [144–146]. At the same time, stronger wave driving in the extratropical mid-to-upper stratosphere accelerates the deep branch of the BDC, enhancing ozone transport into the high-latitude lower stratosphere [147] and strengthening the net STE flux [53,148–150]. The Quasi-Biennial Oscillation (QBO) exerts a modulation on stratospheric ozone in the tropics and mid-latitudes: its easterly

Downloaded from royalsocietypublishing.org/rsta/article-pdf/doi/10.1098/rsta.2025.0271/6174200/rsta.2025.0271.pdf
by Karlsruhe Inst of Technology user
on 02 November 2026

phase enhances poleward and downward transport into the mid-latitudes through the secondary meridional overturning circulation, especially in the winter hemisphere [151]. This can lead to enhanced STT during the easterly phase [152]. ENSO and the QBO can interact, with El Niño events affecting the QBO phases and altering extratropical wave patterns [153,154]. Their nonlinear interactions affect the polar vortex and the BDC and thus modulate ozone transport. The Madden–Julian Oscillation (MJO) further contributes by modulating tropical convection and wave activity on intraseasonal time scales, with convectively active phases enhancing tracer injection and altering tropopause height and structure [155]. Multiple linear regression analysis shows that ENSO, QBO and BDC explain the variance in the global ozone STE monthly anomalies from 1980 to 2022 by 17.3%, 5.4% and 1.0% in ERA5, and by 5.0%, 7.2% and 3.1% in MERRA-2, respectively [7].

Other modes of variability primarily affect regional and episodic exchange via tropopause folds and stratospheric intrusions. ENSO-related wave anomalies modify intrusion frequency across the Pacific–North American sector, with more frequent springtime folds over the North Pacific during La Niña [88,156]. Over the North Atlantic and Europe, the North Atlantic Oscillation (NAO) strongly modulates jet strength and position, enhancing tropopause folding and downward ozone transport during its positive phase and suppressing it during its negative phase [115]. Interactions between ENSO and the NAO can further shape jet variability and ozone intrusions [115]. In the extratropics, the MJO similarly influences jet variability and episodic ozone intrusions [149]. Episodic disturbances provide additional drivers of STE variability. Large volcanic eruptions modify stratospheric radiative heating and circulation, influencing the distribution and downward transport of ozone and water vapour, and can also cause chemical stratospheric ozone destruction in the lower stratosphere [157,158]. Sudden stratospheric warmings enhance ozone STT into the mid- and high-latitude troposphere, with significant anomalies lasting up to three months [159–162].

9. Past changes in stratosphere–troposphere exchange

Multiple lines of evidence show that STE has decreased over the period 1960–2000, which reflects the combined influences of ODS, GHG-induced climate change and variability in tropospheric ozone. The most comprehensive analysis of the drivers of historical STE changes is provided by Wang & Fu [138], who evaluated STE trends derived from ten CCMI-1 chemistry–climate models for this period. Nine of the 10 models show negative STE trends, with a model spread ranging from approximately 1% to −9% decade^{-1} and a multi-model mean of −2.7% decade^{-1}. This decrease in STE was attributed predominantly to the effects of ODS, which reduced lower-stratospheric ozone mixing ratios and hence the ozone mixing ratios in air transported into the troposphere. This effect is partly compensated by GHG-driven climate change, which increases STE through a combination of dynamical and chemical responses, including an acceleration of the BDC and increases in stratospheric ozone linked to cooling of the stratosphere. Attribution of these competing influences was enabled by sensitivity experiments (SEN-C2-fODS and SEN-C2-fGHG) in a subset of the CCMI-1 models, in which ODS or GHGs were held fixed, respectively.

These global results vary significantly by latitude range. Model- and reanalysis-based estimates of STE show regionally distinct trends [1,55,138,143]. In the Northern Hemisphere extratropics, 1960–2000 STE trends are near zero owing to a cancellation between climate-driven increases in transport and ODS-driven ozone depletion, while in the Southern Hemisphere extratropics ODS effects dominated, leading to a strong decrease in STE over the same period [138]. In the tropics, increased transport of ozone from the TST, driven by higher tropospheric ozone concentrations and changes in tropical tropopause height, further reduced the global STE. Derived STE trends over this period also have a strong seasonal cycle, with the strongest decreases occurring in December–February in the extratropics, driven predominantly by large negative trends in the Southern Hemisphere extratropics following the breakup of the Antarctic polar vortex.

Downloaded from royalsocietypublishing.org/rsta/article-pdf/doi/10.1098/rsta.2025.0271/6174200/rsta.2025.0271.pdf
by Karlsruhe Inst of Technology user
on 02 November 2026

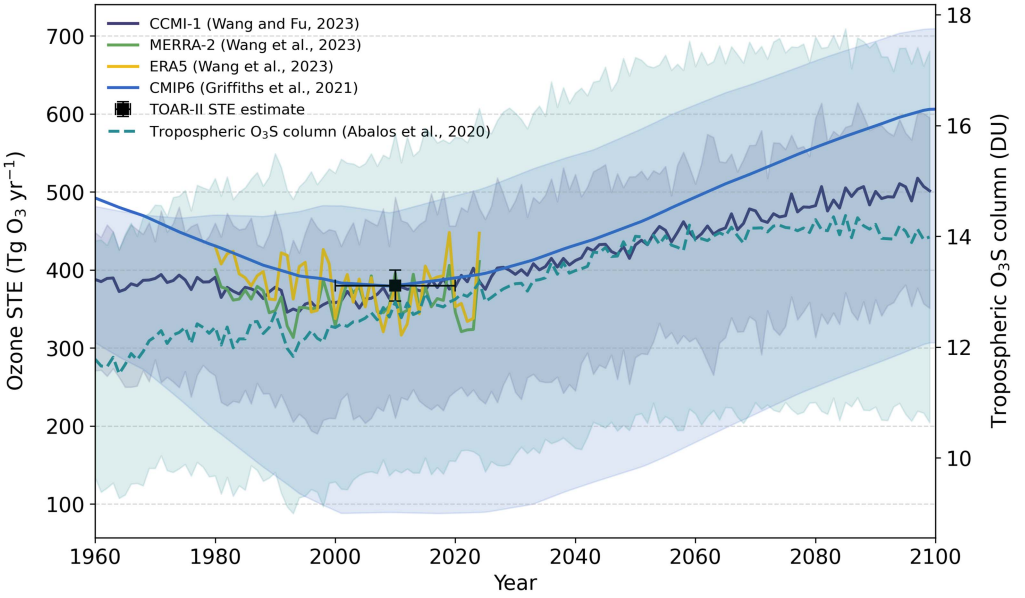


Figure 5. Published transient estimates of ozone STE from CCMI-1 (blue solid line), MERRA-2 (green solid line), ERA5 (yellow solid line) and CMIP6 (olive solid line). The TOAR-2 estimate of ozone STE derived in this study is shown (black square), with the abscissa error bars representing the range of dates for which this estimate is valid (2000–2020). The CCMI-1 and CMIP6 multi-model projections have been adjusted by applying a constant offset so that their 2010 values match the TOAR-2 estimate of STE (380 Tg O_3 yr^{-1}). This adjustment preserves the simulated temporal variability while facilitating comparison with the assessed present-day STE estimate. The blue dashed line shows the tropospheric O_3S column derived from CCMI-1 models, with values shown on the right-hand ordinate. The publications from which these datasets are taken are given in the legend.

10. Projected future changes in stratosphere–troposphere exchange

Chemistry–climate models consistently suggest an increase in STE over the twenty-first century [28,122,125–127,138,140,163–166]. Many model projections use tagged tracers such as O_3S, which consistently show increases in tropospheric columns across models and scenarios, albeit with differences in magnitude [125,126,140,163,164], while budget-based approaches similarly indicate increases [122,138]. Figure 5 shows projections of STE and O_3S changes taken from recently published studies that use different methodologies for determining STE. This increase reflects both rising stratospheric ozone concentrations owing to the recovery of the ozone layer, and dynamical changes such as the acceleration of the BDC and the frequency and depth of tropopause folds in response to GHG changes. To facilitate comparison among datasets with different absolute STE estimates, CCMI-1 and CMIP6 time series were shifted by a constant offset to match the assessed TOAR-2 STE estimate in 2010 (380 Tg O_3 yr^{-1}); this adjustment does not modify their simulated temporal trends. Also shown in figure 5 are STE estimates derived from the MERRA-2 and ERA5 reanalyses, which provide observationally constrained estimates of recent variability and are the same datasets shown in figure 4.

Wang & Fu [138], in their evaluation of STE trends derived from ten CCMI-1 chemistry–climate models, reported a multi-model mean increase in global STE of 4.7% $decade^{-1}$ over the twenty-first century, with a model spread of 3.7–8.9% $decade^{-1}$. These model simulations were conducted using the WMO (2010) A1 scenario for ODS [167] and the RCP 6.0 scenario for other GHGs [168]. As for historical periods, there remains a clear spread across seasonal and regional projected trends. However, in contrast to the late twentieth century, both declining ODS loadings and increasing GHGs act to increase STE. Wang & Fu [138] further show that the GHG-driven component dominates the projected global increase in STE, while ozone recovery provides a secondary but reinforcing contribution. Sensitivity studies suggest that higher-emissions scenarios (i.e. RCP8.5,

Downloaded from royalsocietypublishing.org/rsta/article-pdf/doi/10.1098/rsta.2025.0271/6174200/rsta.2025.0271.pdf
by Karlsruhe Inst of Technology user
on 02 November 2026

SSP5-8.5) yield stronger increases in STE than strong mitigation scenarios, but current evidence is insufficient to establish this response with high confidence [125,127,148].

Despite broad agreement on a future increase in STE, there remain substantial uncertainties in quantifying future changes. These stem from differences in diagnostics, model representations of stratospheric and tropospheric chemistry and transport, and scenario dependence, as well as the limited availability of relevant diagnostics in recent multi-model intercomparisons such as CMIP6. Nonetheless, the consensus across multiple modelling frameworks is that climate change and ozone recovery together will enhance stratospheric contributions to tropospheric ozone throughout the century.

11. Role of stratosphere–troposphere exchange in the tropospheric ozone budget

There has been considerable interest in the role of STE in the tropospheric ozone budget, both over the recent historical period and into the future, given the changes in STE discussed above. The impact of STE on the tropospheric ozone budget is complex. STE primarily acts as a source of ozone, but it can also indirectly influence chemical production and loss mechanisms within the troposphere. Wild [10] estimated that 60% of ozone transported into the troposphere from the stratosphere is chemically destroyed, 10% is removed by dry deposition and 30% replaces ozone that would otherwise have been produced chemically, i.e. net *in situ* ozone production in the troposphere is reduced relative to what it would otherwise be in the absence of the stratospheric ozone source.

In broad terms, the total amount of ozone in the troposphere (the tropospheric ozone burden) is controlled by four main processes: chemical production (Prod), chemical loss (Loss), deposition at the surface (Dep) and STE. Under present-day conditions, multi-model analyses indicate that global tropospheric ozone production is approximately 5000 Tg O_3 yr^{-1} [8,122,138,169], while present-day STE is estimated to be approximately 380 Tg O_3 yr^{-1}. Taken together, these estimates imply that STE accounts for approximately 7% (roughly 6–9% considering the uncertainty in STE and production estimates) of the total tropospheric ozone source under present-day conditions. Although an order of magnitude smaller than gross chemical production, STE is comparable in magnitude to net chemical production (Prod − Loss), meaning it can strongly influence the tropospheric ozone burden despite representing a relatively small fraction of gross ozone production.

The relative importance of STE as a source of tropospheric ozone has not been constant over time. Over the period from 1960 to 2000, STE has declined, primarily owing to ODS–driven reductions in lower-stratospheric ozone, while multi-model studies indicate that tropospheric ozone production has increased substantially owing to rising precursor emissions and climate-driven changes in chemistry [122,138]. As a result, the fractional contribution of STE to the tropospheric ozone source is probably at a multi-decadal minimum in the present climate. In the future, STE is projected to increase over the twenty-first century, while future changes in tropospheric ozone production will depend strongly on emissions pathways and climate state. Under strong mitigation scenarios (e.g. SSP1), in which precursor emissions decline substantially, STE is therefore expected to become an increasingly important relative source of tropospheric ozone. In contrast, under high-emissions scenarios such as SSP5-8.5, large increases in chemical production are likely to limit the relative contribution of STE.

Finally, estimates of the stratospheric contribution to tropospheric ozone depend on the budget framework used. The values discussed above are based on the tropospheric odd-oxygen (Ox) budget framework. Bates & Jacob [169] demonstrated that when using an expanded odd-oxygen (Oy) framework, which makes different assumptions about chemical production and loss terms, the same STE flux of approximately 500 Tg O_3 yr^{-1} corresponds to a substantially larger inferred stratospheric contribution to tropospheric ozone under present-day conditions (26%) compared with estimates derived using the standard Ox budget (9%). The details of the Oy framework are beyond the scope of this assessment (see [169]), but this comparison illustrates that the inferred

Downloaded from royalsocietypublishing.org/rsta/article-pdf/doi/10.1098/rsta.2025.0271/6174200/rsta.2025.0271.pdf
by Karlsruhe Inst of Technology user
on 02 November 2026

importance of STE for the ozone budget depends not only on the transport flux itself, but also on how ozone chemistry is represented within the budget framework.

12. Conclusion

STE represents a persistent, dynamically driven net pathway by which ozone is transported into the troposphere. At monthly-mean and longer time scales, the global pattern of STE is fundamentally governed by the large-scale stratospheric circulation. Tropospheric air masses cross the tropopause in the tropics and ascend through the stratosphere before turning poleward and descending in the extratropics. As a result, the net global ozone flux associated with STE consists of a large positive STT term in the extratropics that is partially offset by a smaller, negative TST term in the tropics. At synoptic spatial scales, processes such as tropopause folding play a key role in episodic ozone transport into the troposphere.

This assessment synthesizes evidence from observations, reanalyses and chemistry–climate models to provide a consistent evaluation of the magnitude, variability and future evolution of STE. Drawing on published STE estimates derived from observational datasets, global reanalyses, single-model studies and multi-model evaluations, this assessment determines a median present-day (2000–2020) global STE of 380 (350–450) Tg O_3 yr^{-1}. The convergence of independent estimates over recent decades indicates that the magnitude of global STE is now reasonably well constrained, with most recent estimates falling within the range 350–550 Tg O_3 yr^{-1}. However, the remaining spread among estimates demonstrates that methodological differences, particularly in the treatment of chemical ozone tendencies and budget closure, remain a major source of uncertainty. Interannual variability in STE is closely linked to modes of climate variability, including ENSO, the QBO, the MJO and the NAO, reflecting the strong dependence of STE on large-scale circulation and wave-driven dynamics.

Chemistry–climate models consistently project an increase in STE over the twenty-first century, driven by stratospheric ozone recovery and GHG-induced circulation changes. A key implication of this assessment is that STE should not be considered a fixed contribution to the tropospheric ozone budget. Instead, its relative importance is expected to increase as stratospheric ozone recovers and as atmospheric circulation responds to increasing GHGs. This projected increase has important implications for the future evolution of tropospheric ozone, with potential consequences for air quality and radiative forcing.

The role of STE in the tropospheric ozone budget depends not only on the magnitude of the ozone flux, but also on where ozone enters the troposphere and how it is subsequently redistributed and removed. Although STE represents only a small fraction of gross tropospheric ozone production, it constitutes an important external source of ozone to the troposphere. However, quantifying its contribution remains sensitive to the budget framework used, highlighting the need for careful interpretation when comparing studies based on different definitions of ozone production, loss and transport.

A key outcome of this assessment is the need for greater care in distinguishing between STT, the one-directional transport from the stratosphere to the troposphere, and STE, the net flux across the tropopause. These terms are frequently used interchangeably in the literature, despite representing distinct quantities. Consistent terminology is essential for interpretation and comparison of results. We recommend that future assessments adopt a consistent convention in which positive STE denotes net transport of ozone into the troposphere.

Finally, this assessment highlights the need for improved diagnostics in multi-model studies. In several recent multi-model assessments, STE estimates have been derived using the residual budget method, and have relied on diagnostics that do not include all of the chemical production and loss processes needed to calculate the residual. As a result, unaccounted-for chemical terms can be incorporated into the inferred STE, contributing to substantial model–model variation. Future multi-model intercomparisons should therefore diagnose the net chemical ozone tendency

Downloaded from royalsocietypublishing.org/rsta/article-pdf/doi/10.1098/rsta.2025.0271/6174200/rsta.2025.0271.pdf
by Karlsruhe Inst of Technology user
on 02 November 2026

explicitly, rather than relying on incomplete production and loss diagnostics. This would allow STE to be diagnosed more robustly without adding significantly to the total number or complexity of model diagnostics.

Ethics. This work did not require ethical approval from a human subject or animal welfare committee.

Data accessibility. There are no primary data associated with this assessment paper. All data in figures and text come from published studies and are referenced [57]. The CAMS global reanalysis (EAC4) data used in figure 1 were provided by the Copernicus Atmosphere Monitoring Service Atmosphere Data Store, DOI: 10.24381/d58bbf47 (last access: 31 December 2025) [170]. The ERA5 data used in figure 1 were provided by the Copernicus Climate Change Service, Climate Data Store, (2023): ERA5 hourly data on single levels from 1940 to present. Copernicus Climate Change Service (C3S) Climate Data Store (CDS). DOI:10.24381/cds.adbb2d47 (last access: 31 December 2025) [171]. The MERRA-2 data used in figure 4 are available via the GES DISC archive, managed by the NASA Goddard Earth Sciences (GES) Data and Information Services Center (DISC). We acknowledge the World Climate Research Programme, which, through its Working Group on Coupled Modelling, coordinated and promoted CMIP6. We thank the climate modelling groups for producing and making available their model output, the Earth System Grid Federation (ESGF) for archiving the data and providing access, and the multiple funding agencies who support CMIP6 and ESGF. The CCMI output data can be downloaded from the Centre for Environmental Data Analysis (CEDA): http://data.ceda.ac.uk/badc/wcrp-ccmi/data/CCMI-1/output/ (last access: 31 December 2025).

Supplementary material is available online [172].

Declaration of AI use. We have not used AI-assisted technologies in creating this article.

Authors' contributions. J.K.: conceptualization, data curation, formal analysis, investigation, methodology, project administration, visualization, writing—original draft, writing—review and editing; P.T.G.: conceptualization, data curation, formal analysis, investigation, methodology, project administration, writing—original draft, writing—review and editing; M.A.: conceptualization, data curation, formal analysis, investigation, methodology, writing—original draft, writing—review and editing; D.A.: conceptualization, data curation, investigation, methodology, project administration, visualization, writing—original draft, writing—review and editing; S.B.: data curation, visualization, writing—original draft, writing—review and editing; O.R.C.: conceptualization, investigation, methodology, writing—original draft, writing—review and editing; Q.F.: conceptualization, data curation, investigation, methodology, writing—original draft, writing—review and editing; M.I.H.: investigation, writing—original draft, writing—review and editing; F.I.-S.: conceptualization, investigation, methodology, writing—original draft, writing—review and editing; G.K.: investigation, methodology, writing—original draft, writing—review and editing; O.N.: investigation, methodology, writing—original draft, writing—review and editing; M.P.: conceptualization, investigation, methodology, writing—original draft, writing—review and editing; D.P.: conceptualization, investigation, methodology, writing—original draft, writing—review and editing; C.R.: investigation, methodology, writing—original draft, writing—review and editing; B.B.S.: investigation, methodology, writing—original draft, writing—review and editing; A.S.: conceptualization, investigation, methodology, writing—original draft, writing—review and editing; K.B.: conceptualization, investigation, methodology, writing—original draft, writing—review and editing; T.T.: investigation, methodology, writing—original draft, writing—review and editing; O.W.: conceptualization, investigation, methodology, writing—original draft, writing—review and editing; P.Z.: conceptualization, investigation, methodology, writing—original draft, writing—review and editing.

All authors gave final approval for publication and agreed to be held accountable for the work performed therein.

Conflict of interest declaration. We declare we have no competing interests.

Funding. Q.F. has been supported by NSF Grants AGS-2202812 and AGS-2531488. O.N. was supported by the Royal Belgian Institute for Space Aeronomy (BIRA-IASB) and the Belgian federal Science Policy Office (BELSPO) through the BRAIN-be 2.0 research project TAPIOWCA (grant B2/223/P1/TAPIOWCA, 2022-2025).

Acknowledgments. The authors acknowledge guidance and support from the International Global Atmospheric Chemistry (IGAC) project. Tropospheric Ozone Assessment Report II (TOAR-II) has been conducted as a sponsored IGAC Activity. M.A. acknowledges funding from the Spanish national project RecO3very (PID2021-124772OB-I00). We would like to thank Anna Hall and Cong Dong for preparing the Wang & Fu [138] data used in several of the plots in this paper. The authors thank the members of the TOAR-II community who contributed constructive comments and feedback during the community review phase prior to submission. We also thank the anonymous reviewers for their constructive and insightful comments, which helped to improve the manuscript.

Downloaded from royalsocietypublishing.org/rsta/article-pdf/doi/10.1098/rsta.2025.0271/6174200/rsta.2025.0271.pdf
by Karlsruhe Inst of Technology user
on 02 November 2026

References

1. Hall A, Fu Q, Dong C. 2025 Revisiting the stratosphere–troposphere exchange of air mass and ozone based on reanalyses and observations. *Atmosphere* **16**, 1050. (doi:10.3390/atmos16091050)
2. Wang M, Fu Q. 2021 Stratosphere-troposphere exchange of air masses and ozone concentrations based on reanalyses and observations. *JGR Atmos.* **126**, e2021JD035159. (doi:10.1029/2021JD035159)
3. Oberländer-Hayn S, Gerber EP, Abalichin J, Akiyoshi H, Kerschbaumer A, Kubin A *et al.* 2016 Is the Brewer-Dobson circulation increasing or moving upward? *Geophys. Res. Lett.* **43**, 1772–1779. (doi:10.1002/2015GL067545)
4. Hall TM, Holzer M. 2003 Advective-diffusive mass flux and implications for stratosphere-troposphere exchange. *Geophys. Res. Lett.* **30**, 2002GL016419. (doi:10.1029/2002GL016419)
5. Griffiths PT, Keeble J, Shin YM, Abraham NL, Archibald AT, Pyle JA. 2020 On the changing role of the stratosphere on the Tropospheric ozone budget: 1979–2010. *Geophys. Res. Lett.* **47**, e2019GL086901. (doi:10.1029/2019GL086901)
6. Ruiz DJ, Prather MJ. 2022 From the middle stratosphere to the surface, using nitrous oxide to constrain the stratosphere–troposphere exchange of ozone. *Atmos. Chem. Phys.* **22**, 2079–2093. (doi:10.5194/acp-22-2079-2022)
7. Wang M, Fu Q, Hall A, Sweeney A. 2023 Stratosphere-troposphere exchanges of air mass and ozone concentrations from ERA5 and MERRA2: annual-mean climatology, seasonal cycle, and interannual variability. *JGR Atmos.* **128**, e2023JD039270. (doi:10.1029/2023JD039270)
8. Young PJ *et al.* 2018 Tropospheric Ozone Assessment Report: assessment of global-scale model performance for global and regional ozone distributions, variability, and trends. *Elem. Sci. Anth.* **6**, 10. (doi:10.1525/elementa.265)
9. Archibald AT *et al.* 2020 Tropospheric Ozone Assessment Report: A critical review of changes in the tropospheric ozone burden and budget from 1850 to 2100. *Elem. Sci. Anth.* **8**, 034. (doi:10.1525/elementa.2020.034)
10. Wild O. 2007 Modelling the global tropospheric ozone budget: exploring the variability in current models. *Atmos. Chem. Phys.* **7**, 2643–2660. (doi:10.5194/acp-7-2643-2007)
11. Stohl A *et al.* 2003 Stratosphere-troposphere exchange: A review, and what we have learned from STACCATO. *J. Geophys. Res.* **108**, 2002JD002490. (doi:10.1029/2002JD002490)
12. Gettelman A, Hoor P, Pan LL, Randel WJ, Hegglin MI, Birner T. 2011 The extratropical upper troposphere and lower stratosphere. *Rev. Geophys.* **49**, 2011RG000355. (doi:10.1029/2011RG000355)
13. Hegglin MI, Boone CD, Manney GL, Walker KA. 2009 A global view of the extratropical tropopause transition layer from Atmospheric Chemistry Experiment fourier transform spectrometer O_3, H_2O, and CO. *J. Geophys. Res.* **114**, 2008JD009984. (doi:10.1029/2008JD009984)
14. Prather MJ, Zhu X, Tang Q, Hsu J, Neu JL. 2011 An atmospheric chemist in search of the tropopause. *J. Geophys. Res.* **116**, D04306. (doi:10.1029/2010JD014939)
15. Danielsen EF. 1968 Stratospheric-tropospheric exchange based on radioactivity, ozone and potential vorticity. *J. Atmos. Sci.* **25**, 502–518. (doi:10.1175/1520-0469(1968)025%3C0502:STEBOR%3E2.0.CO;2)
16. Danielsen EF, Mohnen VA. 1977 Project dustorm report: ozone transport, in situ measurements, and meteorological analyses of tropopause folding. *J. Geophys. Res.* **82**, 5867–5877. (doi:10.1029/JC082i037p05867)
17. Holton JR, Haynes PH, McIntyre ME, Douglass AR, Rood RB, Pfister L. 1995 Stratosphere-troposphere exchange. *Rev. Geophysics* **33**, 403–439. (doi:10.1029/95RG02097)
18. Reed RJ. 1955 A study of A characteristic tpye of upper-level frontogenesis. *J. Meteor.* **12**, 226–237. (doi:10.1175/1520-0469(1955)012%3C0226:ASOACT%3E2.0.CO;2)
19. World Meteorological Organization. 1957 Definition of the tropopause. *Bull. World Meteorol. Organ.* **6**, 136–137.
20. Bethan S, Vaughan G, Reid SJ. 1996 A comparison of ozone and thermal tropopause heights and the impact of tropopause definition on quantifying the ozone content of the troposphere. *Quart. J. R. Meteorol. Soc* **122**, 929–944. (doi:10.1002/qj.49712253207)
21. Homeyer CR, Bowman KP, Pan LL, Zondlo MA, Bresch JF. 2011 Convective injection into stratospheric intrusions. *J. Geophys. Res.* **116**, D23304. (doi:10.1029/2011JD016724)

Downloaded from royalsocietypublishing.org/rsta/article-pdf/doi/10.1098/rsta.2025.0271/6174200/rsta.2025.0271.pdf
by Karlsruhe Inst of Technology user
on 02 November 2026

22. Hoerling MP, Schaack TK, Lenzen AJ. 1991 Global objective tropopause analysis. *Mon. Weather Rev.* **119**, 1816–1831. (doi:10.1175/1520-0493(1991)119⟩1816:GOTA⟩⟨2.0.CO;2)
23. Schoeberl MR. 2004 Extratropical stratosphere-troposphere mass exchange. *J. Geophys. Res.* **109**, 2004JD004525. (doi:10.1029/2004JD004525)
24. Stohl A. 2001 A 1-year lagrangian "climatology" of airstreams in the northern hemisphere troposphere and lowermost stratosphere. *J. Geophys. Res.* **106**, 7263–7279. (doi:10.1029/2000JD900570)
25. Kunz A, Konopka P, Müller R, Pan LL. 2011 Dynamical tropopause based on isentropic potential vorticity gradients. *J. Geophys. Res.* **116**, D01110. (doi:10.1029/2010JD014343)
26. Browell EV *et al.* 1996 Ozone and aerosol distributions and air mass characteristics over the South Atlantic Basin during the burning season. *J. Geophys. Res.* **101**, 24043–24068. (doi:10.1029/95JD02536)
27. Pan LL, Randel WJ, Gary BL, Mahoney MJ, Hintsa EJ. 2004 Definitions and sharpness of the extratropical tropopause: A trace gas perspective. *J. Geophys. Res.* **109**, 2004JD004982. (doi:10.1029/2004JD004982)
28. Young PJ *et al.* 2013 Pre-industrial to end 21st century projections of tropospheric ozone from the Atmospheric Chemistry and Climate Model Intercomparison Project (ACCMIP). *Atmos. Chem. Phys.* **13**, 2063–2090. (doi:10.5194/acp-13-2063-2013)
29. Yang H, Chen G, Tang Q, Hess P. 2016 Quantifying isentropic stratosphere-troposphere exchange of ozone. *JGR Atmos.* **121**, 3372–3387. (doi:10.1002/2015JD024180)
30. Hsu J, Prather MJ, Wild O. 2005 Diagnosing the stratosphere-to-troposphere flux of ozone in a chemistry transport model. *J. Geophys. Res.* **110**, 2005JD006045. (doi:10.1029/2005JD006045)
31. Waugh DW, Funatsu BM. 2003 Intrusions into the tropical upper troposphere: three-dimensional structure and accompanying ozone and OLR distributions. *J. Atmospheric. Sci.* **60**, 637–653. (doi.org/10.1175/1520-0469(2003)060⟨0637:iittut⟩2.0.co;2)
32. Appenzeller C, Holton JR, Rosenlof KH. 1996 Seasonal variation of mass transport across the tropopause. *J. Geophys. Res.* **101**, 15071–15078. (doi:10.1029/96JD00821)
33. Cooper OR *et al.* 2005 Direct transport of midlatitude stratospheric ozone into the lower troposphere and marine boundary layer of the tropical Pacific Ocean. *J. Geophys. Res.* **110**, 2005JD005783. (doi:10.1029/2005JD005783)
34. Gouget H, Vaughan G, Marenco A, Smit HGJ. 2000 Decay of a cut-off low and contribution to stratosphere-troposphere exchange. *Quart. J. R. Meteoro. Soc* **126**, 1117–1141. (doi:10.1002/qj.49712656414)
35. Price JD, Vaughan G. 1993 The potential for stratosphere-troposphere exchange in cut-off-low systems. *Quart. J. R. Meteorol. Soc* **119**, 343–365. (doi:10.1002/qj.49711951007)
36. Škerlak B, Sprenger M, Wernli H. 2014 A global climatology of stratosphere–troposphere exchange using the ERA-Interim data set from 1979 to 2011. *Atmos. Chem. Phys.* **14**, 913–937. (doi:10.5194/acp-14-913-2014)
37. Sprenger M, Croci Maspoli M, Wernli H. 2003 Tropopause folds and cross-tropopause exchange: a global investigation based upon ECMWF analyses for the time period March 2000 to February 2001. *J. Geophys. Res.* **108**, 2002JD002587. (doi:10.1029/2002JD002587)
38. Jaeglé L, Wood R, Wargan K. 2017 Multiyear composite view of ozone enhancements and stratosphere-to-troposphere transport in dry intrusions of Northern hemisphere extratropical cyclones. *JGR Atmos.* **122**. 13,436–13,457 (doi:10.1002/2017JD027656)
39. Keyser D, Shapiro MA. 1986 A review of the structure and dynamics of upper-level frontal zones. *Mon. Wea. Rev.* **114**, 452–499. (doi:10.1175/1520-0493(1986)114%3C0452:AROTSA%3E2.0.CO;2)
40. Knowland KE, Ott LE, Duncan BN, Wargan K. 2017 Stratospheric intrusion-influenced ozone air quality exceedances investigated in the NASA MERRA-2 reanalysis. *Geophys. Res. Lett.* **44**, 10,691–10,701 (doi:10.1002/2017GL074532)
41. Shapiro MA. 1976 The role of turbulent heat flux in the generation of potential vorticity in the vicinity of upper-level jet stream systems. *Monthly Weather Rev.* **104**, 892–906. (doi:10.1175/1520-0493(1976)104%3C0892:TROTHF%3E2.0.CO;2)
42. Shapiro MA. 1980 Turbulent mixing within tropopause folds as a mechanism for the exchange of chemical constituents between the stratosphere and troposphere. *J. Atmos. Sci.* **37**, 994–1004. (doi:10.1175/1520-0469(1980)037%3C0994:TMWTFA%3E2.0.CO;2)
43. Appenzeller C, Davies HC. 1992 Structure of stratospheric intrusions into the troposphere. *Nature* **358**, 570–572. (doi:10.1038/358570a0)

Downloaded from royalsocietypublishing.org/rsta/article-pdf/doi/10.1098/rsta.2025.0271/6174200/rsta.2025.0271.pdf
by Karlsruhe Inst of Technology user
on 02 November 2026

44. Lamarque J-F, Langford AO, Proffitt MH. 1996 Cross-tropopause mixing of ozone through gravity wave breaking: observation and modeling. *J. Geophys. Res.* **101**, 22969–22976. (doi:10.1029/96JD02442)
45. McIntyre ME, Palmer TN. 1983 Breaking planetary waves in the stratosphere. *Nature* **305**, 593–600. (doi:10.1038/305593a0)
46. Roy C, Fadnavis S, Sabin TP. 2021 The stratospheric ozone rich cold intrusion during El-Niño over the Indian region: implication during the Indian summer monsoon. *Intl. J. Climatology* **41**, E233–E248. (doi:10.1002/joc.6680)
47. Tang Q, Prather MJ, Hsu J. 2011 Stratosphere-troposphere exchange ozone flux related to deep convection. *Geophys. Res. Lett.* **38**, L03806. (doi:10.1029/2010GL046039)
48. Pan LL *et al.* 2014 Thunderstorms enhance tropospheric ozone by wrapping and shedding stratospheric air. *Geophys. Res. Lett.* **41**, 7785–7790. (doi:10.1002/2014GL061921)
49. Newell RE *et al.* 1996 Vertical fine-scale atmospheric structure measured from NASA DC-8 during PEM-West A. *J. Geophys. Res.* **101**, 1943–1960. (doi:10.1029/95JD02613)
50. Newell RE, Thouret V, Cho JYN, Stoller P, Marenco A, Smit HG. 1999 Ubiquity of quasi-horizontal layers in the troposphere. *Nature* **398**, 316–319. (doi:10.1038/18642)
51. Trickl T, Couret C, Ries L, Vogelman H-E, Sprenger H. 2023 Zugspitze ozone 1970–2020: the role of stratosphere–troposphere transport. *Atmos. Chem. Phys.* **23**, 8403–8427. (doi:10.5194/acp-23-8403-2023)
52. Trickl T, Vogelmann H, Ries L, Sprenger M. 2020 Very high stratospheric influence observed in the free troposphere over the northern Alps – just a local phenomenon? *Atmos. Chem. Phys.* **20**, 243–266. (doi:10.5194/acp-20-243-2020)
53. Neu JL, Flury T, Manney GL, Santee ML, Livesey NJ, Worden J. 2014 Tropospheric ozone variations governed by changes in stratospheric circulation. *Nat. Geosci.* **7**, 340–344. (doi:10.1038/ngeo2138)
54. Škerlak B, Pfahl S, Sprenger M, Wernli H. 2019 A numerical process study on the rapid transport of stratospheric air down to the surface over western North America and the Tibetan Plateau. *Atmos. Chem. Phys.* **19**, 6535–6549. (doi:10.5194/acp-19-6535-2019)
55. Williams RS, Hegglin MI, Kerridge BJ, Jöckel P, Latter BG, Plummer DA. 2019 Characterising the seasonal and geographical variability in tropospheric ozone, stratospheric influence and recent changes. *Atmos. Chem. Phys.* **19**, 3589–3620. (doi:10.5194/acp-19-3589-2019)
56. Bartusek S, Wu Y, Ting M, Zheng C, Fiore A, Sprenger M, Flemming J. 2023 Higher-resolution tropopause folding accounts for more stratospheric ozone intrusions. *Geophys. Res. Lett.* **50**, e2022GL101690. (doi:10.1029/2022GL101690)
57. Inness A *et al.* 2019 The CAMS reanalysis of atmospheric composition. *Atmos. Chem. Phys.* **19**, 3515–3556. (doi:10.5194/acp-19-3515-2019)
58. Akritidis D, Pozzer A, Flemming J, Inness A, Zanis P. 2021 A global climatology of tropopause folds in CAMS and MERRA-2 reanalyses. *JGR Atmos.* **126**, e2020JD034115. (doi:10.1029/2020JD034115)
59. Akritidis D, Pozzer A, Zanis P, Tyrlis E, Škerlak B, Sprenger M, Lelieveld J. 2016 On the role of tropopause folds in summertime tropospheric ozone over the eastern Mediterranean and the Middle East. *Atmos. Chem. Phys.* **16**, 14025–14039. (doi:10.5194/acp-16-14025-2016)
60. Zanis P, Hadjinicolaou P, Pozzer A, Tyrlis E, Dafka S, Mihalopoulos N, Lelieveld J. 2014 Summertime free-tropospheric ozone pool over the eastern Mediterranean/Middle East. *Atmos. Chem. Phys.* **14**, 115–132. (doi:10.5194/acp-14-115-2014)
61. Langford AO, Aikin KC, Eubank CS, Williams EJ. 2009 Stratospheric contribution to high surface ozone in Colorado during springtime. *Geophys. Res. Lett.* **36**. L12801. (doi:10.1029/2009GL038367)
62. Langford AO, Masters CD, Proffitt MH, Hsie E-Y, Tuck AF. 1996 Ozone measurements in a tropopause fold associated with a cut-off low system. *Geophys. Res. Lett.* **23**, 2501–2504. (doi:10.1029/96GL02227)
63. Langford AO, Reid SJ. 1998 Dissipation and mixing of a small-scale stratospheric intrusion in the upper troposphere. *J. Geophys. Res.* **103**, 31265–31276. (doi:10.1029/98JD02596)
64. Lefohn AS, Wernli H, Shadwick D, Limbach S, Oltmans SJ, Shapiro M. 2011 The importance of stratospheric–tropospheric transport in affecting surface ozone concentrations in the western and northern tier of the United States. *Atmos. Environ.* **45**, 4845–4857. (doi:10.1016/j.atmosenv.2011.06.014)

Downloaded from royalsocietypublishing.org/rsta/article-pdf/doi/10.1098/rsta.2025.0271/6174200/rsta.2025.0271.pdf
by Karlsruhe Inst of Technology user
on 02 November 2026

65. Chen XL, Ma YM, Kelder H, Su Z, Yang K. 2011 On the behaviour of the tropopause folding events over the Tibetan Plateau. *Atmos. Chem. Phys.* **11**, 5113–5122. (doi:10.5194/acp-11-5113-2011)
66. Chen X, Añel JA, Su Z, De La Torre L, Kelder H, Van Peet J, Ma Y. 2013 The deep atmospheric boundary layer and its significance to the stratosphere and troposphere exchange over the Tibetan plateau. *PLoS ONE* **8**, e56909. (doi:10.1371/journal.pone.0056909)
67. Stohl A *et al.* 2000 The influence of stratospheric intrusions on alpine ozone concentrations. *Atmos. Environ.* **34**, 1323–1354. (doi:10.1016/S1352-2310(99)00320-9)
68. Zanis P *et al.* 2003 An estimate of the impact of stratosphere-to-troposphere transport (STT) on the lower free tropospheric ozone over the Alps using10 Be and7 Be measurements. *J. Geophys. Res.* **108**, 2002JD002604. (doi:10.1029/2002JD002604)
69. Büker ML, Hitchman MH, Tripoli GJ, Pierce RB, Browell EV, Avery MA. 2005 Resolution dependence of cross-tropopause ozone transport over east Asia. *J. Geophys. Res.* **110**, 2004JD004739. (doi:10.1029/2004JD004739)
70. Spreitzer E, Attinger R, Boettcher M, Forbes R, Wernli H, Joos H. 2019 Modification of potential vorticity near the tropopause by nonconservative processes in the ECMWF model. *J. Atmos. Sci.* **76**, 1709–1726. (doi:10.1175/JAS-D-18-0295.1)
71. Gordon AE, Homeyer CR. 2025 Examining stratosphere-troposphere exchange in an idealized simulation of a tropical cyclone. *JGR Atmos.* **130**, e2025JD044044. (doi:10.1029/2025JD044044)
72. Homeyer CR *et al.* 2014 Convective transport of water vapor into the lower stratosphere observed during double-tropopause events. *J. Geophys. Res. Atmos.* **119**, 10,941-10,958. (doi:10.1002/2014JD021485)
73. Ray EA, Rosenlof KH. 2007 Hydration of the upper troposphere by tropical cyclones. *J. Geophys. Res.* **112**, 2006JD008009. (doi:10.1029/2006JD008009)
74. Roy C *et al.* 2023 Estimation of stratospheric intrusions during indian cyclones. *JGR Atmos.* **128**, e2022JD037519. (doi:10.1029/2022JD037519)
75. Zheng X, Yang WX, Sun Y, Geng C, Liu Y, Xu X 2024 Comment on "Transport of substantial stratospheric ozone to the surface by a dying typhoon and shallow convection". by Chen *et al*. (2022). *Atmos. Chem. Phys.* **24**, 3759–3768. (doi:10.5194/acp-24-3759-2024)
76. Chen Z, Liu J, Qie X, Cheng X, Shen M, Yang M, Jiang R, Liu X. 2022 Transport of substantial stratospheric ozone to the surface by a dying typhoon and shallow convection. *Atmos. Chem. Phys*. **22**, 8221–8240. (doi:10.5194/acp-22-8221-2022)
77. Gaudel A *et al.* 2018 Tropospheric Ozone Assessment Report: present-day distribution and trends of tropospheric ozone relevant to climate and global atmospheric chemistry model evaluation. *Elem. Sci. Anth.* **6**, 39. (doi:10.1525/elementa.291)
78. Akritidis D, Pozzer A, Flemming J, Inness A, Nédélec P, Zanis P. 2022 A process-oriented evaluation of CAMS reanalysis ozone during tropopause folds over Europe for the period 2003–2018. *Atmos. Chem. Phys.* **22**, 6275–6289. (doi:10.5194/acp-22-6275-2022)
79. Trickl T, Vogelmann H, Giehl H, Scheel H-E, Sprenger M, Stohl A. 2014 How stratospheric are deep stratospheric intrusions? *Atmos. Chem. Phys.* **14**, 9941–9961. (doi:10.5194/acp-14-9941-2014)
80. Bithell M, Vaughan G, Gray LJ. 2000 Persistence of stratospheric ozone layers in the troposphere. *Atmos. Environ.* **34**, 2563–2570. (doi:10.1016/S1352-2310(99)00497-5)
81. Forster C, Wirth V. 2000 Radiative decay of idealized stratospheric filaments in the troposphere. *J. Geophys. Res.* **105**, 10169–10184. (doi:10.1029/2000JD900052)
82. Thomas Biyo, Kunchala RK. 2025 Rossby wave breaking and its impact on tropospheric ozone variability over the Indian subcontinent. *Atmos. Environ*. **343**, 120962. (doi:10.1016/j.atmosenv.2024.120962)
83. Akritidis D, Zanis P, Pytharoulis I, Mavrakis A, Karacostas Th. 2010 A deep stratospheric intrusion event down to the earth's surface of the megacity of Athens. *Meteorol. Atmos. Phys.* **109**, 9–18. (doi:10.1007/s00703-010-0096-6)
84. Cooper OR *et al.* 2011 Measurement of western U.S. baseline ozone from the surface to the tropopause and assessment of downwind impact regions: measurement of western U.S. baseline ozone. *J. Geophys. Res.* **116**. D00V03. (doi:10.1029/2011JD016095)
85. Davies TD, Schuepbach E. 1994 Episodes of high ozone concentrations at the earth's surface resulting from transport down from the upper troposphere/lower stratosphere: a review and case studies. *Atmos. Environ.* **28**, 53–68. (doi:10.1016/1352-2310(94)90022-1)

Downloaded from royalsocietypublishing.org/rsta/article-pdf/doi/10.1098/rsta.2025.0271/6174200/rsta.2025.0271.pdf
by Karlsruhe Inst of Technology user
on 02 November 2026

86. Gerasopoulos E, Zanis P, Papastefanou C, Zerefos CS, Ioannidou A, Wernli H. 2006 A complex case study of down to the surface intrusions of persistent stratospheric air over the Eastern Mediterranean. *Atmos. Environ.* **40**, 4113–4125. (doi:10.1016/j.atmosenv.2006.03.022)
87. Lin M *et al.* 2012 Springtime high surface ozone events over the western United States: quantifying the role of stratospheric intrusions. *J. Geophys. Res.* **117**, 2012JD018151. (doi:10.1029/2012JD018151)
88. Lin M, Fiore AM, Horowitz LW, Langford AO, Oltmans SJ, Tarasick D, Rieder HE. 2015 Climate variability modulates western US ozone air quality in spring via deep stratospheric intrusions. *Nat. Commun* **6**, 7105. (doi:10.1038/ncomms8105)
89. Thompson AM *et al.* 2007 Intercontinental Chemical Transport Experiment Ozonesonde Network Study (IONS) 2004: 2. Tropospheric ozone budgets and variability over northeastern North America. *J. Geophys. Res.* **112**, 2006JD007670. (doi:10.1029/2006JD007670)
90. Tarasick DW *et al.* 2019 Quantifying stratosphere-troposphere transport of ozone using balloon-borne ozonesondes, radar windprofilers and trajectory models. *Atmos. Environ.* **198**, 496–509. (doi:10.1016/j.atmosenv.2018.10.040)
91. Dibb JE, Dibb JE, Meeker LD, Finkel RC, Southon JR, Caffee MW, Barrie LA 1994 Estimation of stratospheric input to the Arctic troposphere: 7Be and 10Be in aerosols at Alert, *Canada. J. Geophys. Res.* **99**, 12855–12864. (doi:10.1029/94JD00742)
92. Ott LE *et al.* 2016 Frequency and impact of summertime stratospheric intrusions over Maryland during DISCOVER-AQ (2011): new evidence from NASA's GEOS-5 simulations. *JGR Atmos.* **121**, 3687–3706. (doi:10.1002/2015JD024052)
93. Cristofanelli P, Bonasoni P, Tositti L, Bonafè U, Calzolari F, Evangelisti F, Sandrini S, Stohl A. 2006 A 6-year analysis of stratospheric intrusions and their influence on ozone at Mt. Cimone (2165 m above sea level). *J. Geophys. Res.* **111**, 2005JD006553. (doi:10.1029/2005JD006553)
94. Cristofanelli P *et al.* 2010 Tropospheric ozone variations at the Nepal Climate Observatory-Pyramid (Himalayas, 5079 m a.s.l.) and influence of deep stratospheric intrusion events. *Atmos. Chem. Phys.* **10**, 6537–6549. (doi:10.5194/acp-10-6537-2010)
95. Putero D, Cristofanelli P, Sprenger M, Škerlak B, Tositti L, Bonasoni P. 2016 STEFLUX, a tool for investigating stratospheric intrusions: application to two WMO/GAW global stations. *Atmos. Chem. Phys.* **16**, 14203–14217. (doi:10.5194/acp-16-14203-2016)
96. Trisolino P, Putero D, Arduini J, Amendola S, Calzolari F, Cristofanelli P. 2024 Influence of deep stratosphere-to-troposphere transport on atmospheric carbon dioxide and methane at the Mt. Cimone WMO/GAW global station (2165 m a.s.l., Italy): A multi-year (2015–2022) investigation. *Atmos. Res.* **310**, 107627. (doi:10.1016/j.atmosres.2024.107627)
97. Zanis P *et al.* 2003 Forecast, observation and modelling of a deep stratospheric intrusion event over Europe. *Atmos. Chem. Phys.* **3**, 763–777. (doi:10.5194/acp-3-763-2003)
98. Ambrose JL, Reidmiller DR, Jaffe DA. 2011 Causes of high O3 in the lower free troposphere over the Pacific Northwest as observed at the Mt. Bachelor Observatory. *Atmos. Environ.* **45**, 5302–5315. (doi:10.1016/j.atmosenv.2011.06.056)
99. Mkololo T, Mbatha N, Sivakumar V, Bègue N, Coetzee G, Labuschagne C. 2020 Stratosphere–Troposphere exchange and O3 variability in the lower Stratosphere and upper Troposphere over the Irene SHADOZ Site, South Africa. *Atmosphere* **11**, 586. (doi:10.3390/atmos11060586)
100. Yin X *et al.* 2023 Surface ozone over the Tibetan Plateau controlled by stratospheric intrusion. *Atmos. Chem. Phys.* **23**, 10137–10143. (doi:10.5194/acp-23-10137-2023)
101. Ma X, Huang J, Hegglin MI, Jöckel P, Zhao T. 2025 Causes of growing middle-to-upper tropospheric ozone over the northwest Pacific region. *Atmos. Chem. Phys.* **25**, 943–958. (doi:10.5194/acp-25-943-2025)
102. Meng K, Zhao T, Bai Y, Wu M, Cao L, Hou X, Luo Y, Jiang Y. 2024 Tracing the origins of stratospheric ozone intrusions: direct vs. indirect pathways and their impacts on Central and Eastern China in spring–summer 2019. *Atmos. Chem. Phys.* **24**, 12623–12642. (doi:10.5194/acp-24-12623-2024)
103. Eisele H, Scheel HE, Sladkovic R, Trickl T. 1999 High-resolution lidar measurements of stratosphere–troposphere exchange. *J. Atmos. Sci.* **56**, 319–330. (doi:10.1175/1520-0469(1999)056%3C0319:HRLMOS%3E2.0.CO;2)
104. Galani E, Balis D, Zanis P, Zerefos C, Papayannis A, Wernli H, Gerasopoulos E. 2003 Observations of stratosphere-to-troposphere transport events over the eastern Mediterranean using a ground-based lidar system. *J. Geophys. Res.* **108**, 2002JD002596. (doi:10.1029/2002JD002596)

Downloaded from royalsocietypublishing.org/rsta/article-pdf/doi/10.1098/rsta.2025.0271/6174200/rsta.2025.0271.pdf
by Karlsruhe Inst of Technology user
on 02 November 2026

105. Papayannis A, Balis D, Zanis P, Galani E, Wernli H, Zerefos C, Stohl A, Eckhardt S, Amiridis V. 2005 Sampling of an STT event over the Eastern Mediterranean region by lidar and electrochemical sonde. *Ann. Geophys.* **23**, 2039–2050. (doi:10.5194/angeo-23-2039-2005)
106. Trickl T, Bärtsch-Ritter N, Eisele H, Furger M, Mücke R, Sprenger M, Stohl A. 2011 High-ozone layers in the middle and upper troposphere above Central Europe: potential import from the stratosphere along the subtropical jet stream. *Atmos. Chem. Phys.* **11**, 9343–9366. (doi:10.5194/acp-11-9343-2011)
107. Seguel RJ *et al.* 2025 Hemispheric differences in ozone across the stratosphere–troposphere exchange region. *Atmos. Chem. Phys.* **25**, 8553–8573. (doi:10.5194/acp-25-8553-2025)
108. Olsen MA, Douglass AR, Kaplan TB. 2013 Variability of extratropical ozone stratosphere–troposphere exchange using microwave limb sounder observations. *JGR Atmos.* **118**, 1090–1099. (doi:10.1029/2012JD018465)
109. Olsen MA, Schoeberl MR, Douglass AR. 2004 Stratosphere-troposphere exchange of mass and ozone. *J. Geophys. Res.* **109**, 2004JD005186. (doi:10.1029/2004JD005186)
110. Wang M, Fu Q, Solomon S, Alexander B, White RH. 2022 Stratosphere-troposphere exchanges of air mass and ozone concentration in the last glacial maximum. *JGR Atmos.* **127**, e2021JD036327. (doi:10.1029/2021JD036327)
111. Lin M, Zhang Z, Su L, Su B, Liu L, Tao J, Fung JCH, Thiemens MH. 2016 Unexpected high ^{35}S concentration revealing strong downward transport of stratospheric air during the monsoon transitional period in East Asia. *Geophys. Res. Lett.* **43**, 2315–2322. (doi:10.1002/2016GL068194)
112. Jordan CE, Dibb JE, Finkel RC. 2003 $^{10}Be/^{7}Be$ tracer of atmospheric transport and stratosphere-troposphere exchange. *J. Geophys. Res.* **108**, 2002JD002395. (doi:10.1029/2002JD002395)
113. Adnew GA, Koren G, Mehendale N, Gromov S, Krol M, Röckmann T. 2025 Triple oxygen isotope composition of CO2 in the upper troposphere and stratosphere. *Atmos. Meas. Tech.* **18**, 2701–2719. (doi:10.5194/amt-18-2701-2025)
114. Steur PM, Scheeren HA, Koren G, Adnew GA, Peters W, Meijer HAJ. 2024 Interannual variations in the Δ (17 O) signature of atmospheric CO2 at two mid-latitude sites suggest a close link to stratosphere–troposphere exchange. *Atmos. Chem. Phys.* **24**, 11005–11027. (doi:10.5194/acp-24-11005-2024)
115. Sprenger M, Wernli H. 2003 A northern hemispheric climatology of cross-tropopause exchange for the ERA15 time period (1979–1993). *J. Geophys. Res.* **108**, 2002JD002636. (doi:10.1029/2002JD002636)
116. Staley DO. 1962 On the mechanism of mass and radioactivity transport from stratosphere to troposphere. *J. Atmos. Sci.* **19**, 450–467. (doi:10.1175/1520-0469(1962)019%3C0450:OTMOMA%3E2.0.CO;2)
117. Seo K, Bowman KP. 2001 A climatology of isentropic cross-tropopause exchange. *J. Geophys. Res.* **106**, 28159–28172. (doi:10.1029/2000JD000295)
118. Schoeberl MR, Ueyama R, Pfister L. 2022 A lagrangian view of seasonal stratosphere-troposphere exchange. *JGR Atmos* **127**, e2022JD036772. (doi:10.1029/2022JD036772)
119. Sprenger M, Wernli H, Bourqui M. 2007 Stratosphere–Troposphere exchange and its relation to potential vorticity streamers and cutoffs near the extratropical tropopause. *J. Atmos. Sci.* **64**, 1587–1602. (doi:10.1175/JAS3911.1)
120. Orbe C, Holzer M, Polvani LM. 2012 Flux distributions as robust diagnostics of stratosphere-troposphere exchange. *J. Geophys. Res.* **117**, 2011JD016455. (doi:10.1029/2011JD016455)
121. Wernli H, Bourqui M 2002 A Lagrangian "1-year climatology" of (deep) cross-tropopause exchange in the extratropical Northern Hemisphere. *J. Geophys. Res.* **107**, 4021. (doi:10.1029/2001JD000812)
122. Griffiths PT *et al.* 2021 Tropospheric ozone in CMIP6 simulations. *Atmos. Chem. Phys.* **21**, 4187–4218. (doi:10.5194/acp-21-4187-2021)
123. Wei M-Y. 1987 A new formulation of the exchange of mass and trace constituents between the stratosphere and troposphere. *J. Atmos. Sci.* **44**, 3079–3086. (doi:10.1175/1520-0469(1987)044%3C3079:ANFOTE%3E2.0.CO;2)
124. Wirth V, Egger J. 1999 Diagnosing extratropical synoptic-scale stratosphere-troposphere exchange: a case study. *Quart. J. R. Meteorol. Soc.* **125**, 635–655. (doi:10.1002/qj.49712555413)
125. Abalos M *et al.* 2020 Future trends in stratosphere-to-troposphere transport in CCMI models. *Atmos. Chem. Phys.* **20**, 6883–6901. (doi:10.5194/acp-20-6883-2020)

Downloaded from royalsocietypublishing.org/rsta/article-pdf/doi/10.1098/rsta.2025.0271/6174200/rsta.2025.0271.pdf
by Karlsruhe Inst of Technology user
on 02 November 2026

126. Banerjee A, Maycock AC, Archibald AT, Abraham NL, Telford P, Braesicke P, Pyle JA. 2016 Drivers of changes in stratospheric and tropospheric ozone between year 2000 and 2100. *Atmos. Chem. Phys.* **16**, 2727–2746. (doi:10.5194/acp-16-2727-2016)
127. Meul S, Langematz U, Kröger P, Oberländer-Hayn S, Jöckel P. 2018 Future changes in the stratosphere-to-troposphere ozone mass flux and the contribution from climate change and ozone recovery. *Atmos. Chem. Phys.* **18**, 7721–7738. (doi:10.5194/acp-18-7721-2018)
128. Sudo K, Akimoto H. 2007 Global source attribution of tropospheric ozone: long-range transport from various source regions. *J. Geophys. Res.* **112**, 2006JD007992. (doi:10.1029/2006JD007992)
129. Roelofs G-J, Lelieveld J. 1997 Model study of the influence of cross-tropopause O_3 transports on tropospheric O_3 levels. *Tellus B* **49**, 38–55. (doi:10.1034/j.1600-0889.49.issue1.3.x)
130. Meul S, Dameris M, Langematz U, Abalichin J, Kerschbaumer A, Kubin A, Oberländer-Hayn S. 2016 Impact of rising greenhouse gas concentrations on future tropical ozone and UV exposure. *Geophys. Res. Lett.* **43**, 2919–2927. (doi:10.1002/2016GL067997)
131. Zanis P *et al.* 2022 Climate change penalty and benefit on surface ozone: a global perspective based on CMIP6 earth system models. *Environ. Res. Lett.* **17**, 024014. (doi:10.1088/1748-9326/ac4a34)
132. Prather MJ, Zhu X. 2024 Lifetimes and timescales of tropospheric ozone. *Elem. Sci. Anth.* **12**, 00112. (doi:10.1525/elementa.2023.00112)
133. Fabian P, Pruchniewicz PG. 1977 Meridional distribution of ozone in the troposphere and its seasonal variations. *J. Geophys. Res.* **82**, 2063–2073. (doi:10.1029/JC082i015p02063)
134. Junge CE. 1962 Global ozone budget and exchange between stratosphere and troposphere. *Tellus* **14**, 363–377. (doi:10.1111/j.2153-3490.1962.tb01349.x)
135. Gettelman A, Holton JR, Rosenlof KH. 1997 Mass fluxes of O_3, CH_4, N_2O and CF_2Cl_2 in the lower stratosphere calculated from observational data. *J. Geophys. Res.* **102**, 19149–19159. (doi:10.1029/97JD01014)
136. Murphy DM, Fahey DW. 1994 An estimate of the flux of stratospheric reactive nitrogen and ozone into the troposphere. *J. Geophys. Res.* **99**, 5325–5332. (doi:10.1029/93JD03558)
137. Olsen SC, McLinden CA, Prather MJ. 2001 Stratospheric N_2O–NO_y system: testing uncertainties in a three-dimensional framework. *J. Geophys. Res.* **106**, 28771–28784. (doi:10.1029/2001JD000559)
138. Wang M, Fu Q. 2023 Changes in stratosphere-troposphere exchange of air mass and ozone concentration in CCMI models from 1960 to 2099. *JGR Atmos.* **128**, e2023JD038487. (doi:10.1029/2023JD038487)
139. Hu L, Jacob DJ, Liu X, Zhang Y, Zhang L, Kim PS, Sulprizio MP, Yantosca RM. 2017 Global budget of tropospheric ozone: evaluating recent model advances with satellite (OMI), aircraft (IAGOS), and ozonesonde observations. *Atmos. Environ.* **167**, 323–334. (doi:10.1016/j.atmosenv.2017.08.036)
140. Iglesias-Suarez F, Kinnison DE, Rap A, Maycock AC, Wild O, Young PJ. 2018 Key drivers of ozone change and its radiative forcing over the 21st century. *Atmos. Chem. Phys.* **18**, 6121–6139. (doi:10.5194/acp-18-6121-2018)
141. Stevenson DS *et al.* 2006 Multimodel ensemble simulations of present-day and near-future tropospheric ozone. *J. Geophys. Res.* **111**, 2005JD006338. (doi:10.1029/2005JD006338)
142. Abalos M, Ploeger F, Konopka P, Randel WJ, Serrano E. 2013 Ozone seasonality above the tropical tropopause: reconciling the Eulerian and Lagrangian perspectives of transport processes. *Atmos. Chem. Phys.* **13**, 10787–10794. (doi:10.5194/acp-13-10787-2013)
143. Hegglin MI, Shepherd TG. 2009 Large climate-induced changes in ultraviolet index and stratosphere-to-troposphere ozone flux. *Nat. Geosci.* **2**, 687–691. (doi:10.1038/ngeo604)
144. Calvo N, Garcia RR, Randel WJ, Marsh DR. 2010 Dynamical mechanism for the increase in tropical upwelling in the lowermost tropical stratosphere during warm ENSO events. *J. Atmos. Sci.* **67**, 2331–2340. (doi:10.1175/2010JAS3433.1)
145. Diallo M, Konopka P, Santee ML, Muller R, Tao MC, Walker KA, Legras B, Riese M, Ern M, Ploeger F. 2019 Structural changes in the shallow and transition branch of the Brewer-Dobson circulation induced by El Niño. *Atmos. Chem. Phys.* **19**, 425–446. ((doi:10.5194/acp-19-425-2019)
146. Randel WJ, Garcia RR, Calvo N, Marsh D. 2009 ENSO influence on zonal mean temperature and ozone in the tropical lower stratosphere. *Geophys. Res. Lett.* **36**, 2009GL039343. (doi:10.1029/2009GL039343)

Downloaded from royalsocietypublishing.org/rsta/article-pdf/doi/10.1098/rsta.2025.0271/6174200/rsta.2025.0271.pdf
by Karlsruhe Inst of Technology user
on 02 November 2026

147. Benito-Barca S, Calvo N, Abalos M. 2022 Driving mechanisms for the El Niño–Southern Oscillation impact on stratospheric ozone. *Atmos. Chem. Phys.* **22**, 15729–15745. (doi:10.5194/acp-22-15729-2022)
148. Albers JR, Butler AH, Langford AO, Elsbury D, Breeden ML. 2022 Dynamics of ENSO-driven stratosphere-to-troposphere transport of ozone over North America. *Atmos. Chem. Phys.* **22**, 13035–13048. (doi:10.5194/acp-22-13035-2022)
149. Albers JR, Perlwitz J, Butler AH, Birner T, Kiladis GN, Lawrence ZD, Manney GL, Langford AO, Dias J. 2018 Mechanisms governing interannual variability of stratosphere-to-troposphere ozone transport. *JGR Atmos.* **123**, 234–260. (doi:10.1002/2017JD026890)
150. Zeng G, Pyle JA. 2005 Influence of El Niño Southern Oscillation on stratosphere/troposphere exchange and the global tropospheric ozone budget. *Geophys. Res. Lett.* **32**, 2004GL021353. (doi:10.1029/2004GL021353)
151. Baldwin MP *et al.* 2001 The quasi-biennial oscillation. *Rev. Geophys.* **39**, 179–229. (doi:10.1029/1999RG000073)
152. Zhang Z, Liang J, Luo J. 2025 Impacts of the Quasi-Biennial Oscillation and the El Niño-Southern Oscillation on stratosphere-to-troposphere ozone transport: assessment with chemistry-climate models. *J. Geophys. Res. Atmos.* **130**, e2024JD041825 (doi:10.1029/2024JD041825)
153. Olsen MA, Manney GL, Liu J. 2019. The ENSO and QBO impact on ozone variability and stratosphere-troposphere exchange relative to the subtropical jets. *J. Geophys. Res. Atmos.* **124**, 7379–7392. (doi:10.1029/2019JD030435)
154. Taguchi M. 2010 Observed connection of the stratospheric quasi-biennial oscillation with El Niño–Southern Oscillation in radiosonde data. *J. Geophys. Res.* **115**, 2010JD014325. (doi:10.1029/2010JD014325)
155. Randel WJ, Jensen EJ. 2013 Physical processes in the tropical tropopause layer and their roles in a changing climate. *Nat. Geosci.* **6**, 169–176. (doi:10.1038/ngeo1733)
156. Breeden ML, Butler AH, Albers JR, Sprenger M, Langford AO. 2021 The spring transition of the North Pacific jet and its relation to deep stratosphere-to-troposphere mass transport over western North America. *Atmos. Chem. Phys.* **21**, 2781–2794. (doi:10.5194/acp-21-2781-2021)
157. Evan S *et al.* 2023 Rapid ozone depletion after humidification of the stratosphere by the Hunga Tonga Eruption. *Science*, **382**, eadg2551. (doi:10.1126/science.adg2551)
158. Fueglistaler S, Haynes PH. 2005 Control of interannual and longer-term variability of stratospheric water vapor. *J. Geophys. Res.* **110**, 2005JD006019. (doi:10.1029/2005JD006019)
159. De La Cámara A, Abalos M, Hitchcock P, Calvo N, Garcia RR. 2018 Response of Arctic ozone to sudden stratospheric warmings. *Atmos. Chem. Phys.* **18**, 16499–16513. (doi:10.5194/acp-18-16499-2018)
160. Lee J, Butler AH, Albers JR, Wu Y, Lee SH. 2025 Impact of sudden stratospheric warmings on the stratosphere-to-troposphere transport of ozone. *Geophys. Res. Lett.* **52**, e2024GL112588. (doi:10.1029/2024GL112588)
161. Williams RS, Hegglin MI, Jöckel P, Garny H, Shine KP. 2024 Air quality and radiative impacts of downward-propagating sudden stratospheric warmings (SSWs). *Atmos. Chem. Phys.* **24**, 1389–1413. (doi:10.5194/acp-24-1389-2024)
162. Xia Y, Xie F, Lu X. 2023 Enhancement of Arctic surface ozone during the 2020–2021 winter associated with the sudden stratospheric warming. *Environ. Res. Lett.* **18**, 024003. (doi:10.1088/1748-9326/acaee0)
163. Akritidis D, Pozzer A, Zanis P. 2019 On the impact of future climate change on tropopause folds and tropospheric ozone. *Atmos. Chem. Phys.* **19**, 14387–14401. (doi:10.5194/acp-19-14387-2019)
164. Elsbury D, Butler AH, Albers JR, Breeden ML, Langford AO. 2023 The response of the North Pacific jet and stratosphere-to-troposphere transport of ozone over western North America to RCP8.5 climate forcing. *Atmos. Chem. Phys.* **23**, 5101–5117. (doi:10.5194/acp-23-5101-2023)
165. Kawase H, Nagashima T, Sudo K, Nozawa T. 2011 Future changes in tropospheric ozone under representative concentration pathways (RCPs): changes in tropospheric ozone under RCPs. *Geophys. Res. Lett.* **38**, n/a–n/a. (doi:10.1029/2010GL046402)
166. Collins WJ, Derwent RG, Garnier B, Johnson CE, Sanderson MG, Stevenson DS. 2003 Effect of stratosphere-troposphere exchange on the future tropospheric ozone trend. *J. Geophys. Res.* **108**, 2002JD002617. (doi:10.1029/2002JD002617)

Downloaded from royalsocietypublishing.org/rsta/article-pdf/doi/10.1098/rsta.2025.0271/6174200/rsta.2025.0271.pdf
by Karlsruhe Inst of Technology user
on 02 November 2026

167. World Meteorological Organization. 2011 Scientific Assessment of Ozone Depletion: 2010. Global Ozone Research and Monitoring Project-Report No. 52 Geneva, Switzerland: World Meteorological Organization, 516 pp.
168. Meinshausen M *et al.* 2011 The RCP greenhouse gas concentrations and their extensions from 1765 to 2300. *Climatic Change* **109**, 213. (doi:10.1007/s10584-011-0156-z)
169. Bates KH, Jacob DJ. 2020 An expanded definition of the odd oxygen Family for tropospheric ozone budgets: implications for ozone lifetime and stratospheric influence. *Geophys. Res. Lett.* **47**, e2019GL084486. (doi:10.1029/2019GL084486)
170. Hersbach H *et al.* 2023 ERA5 hourly data on single levels from 1940 to present. Copernicus Climate Change Service (C3S) Climate Data Store (CDS).
171. Gelaro R *et al*. 2017 The Modern-Era retrospective analysis for research and applications, version 2 (MERRA-2). *Journal of Climate*, **30**, 5419–5454. (doi:10.1175/jcli-d-16-0758.1)
172. Keeble J *et al.* 2026 Supplementary material from: Tropospheric Ozone Assessment Report II: Stratosphere–troposphere exchange of ozone. Figshare. (doi:10.6084/m9.figshare.c.8658118)

Downloaded from royalsocietypublishing.org/rsta/article-pdf/doi/10.1098/rsta.2025.0271/6174200/rsta.2025.0271.pdf
by Karlsruhe Inst of Technology user
on 02 November 2026